SEISMIC ASSESSMENT OF A MASONRY CHURCH AND RETROFITTING PROPOSITIONS

Case study of the Kapela Sveti Nikola in Petrinja

Master thesis

Melchior Frick

June 23, 2023

Prof. Katrin Beyer
Dr. Igor Tomic
Dr. Savvas Saloustros

Abstract

The seismic assessment of historical unreinforced masonry buildings is a challenging task, because of their vulnerability to earthquakes and the uncertainties about the material properties. This work studies the case of the Kapela Sveti Nikola, a chapel in Petrinja (Croatia) which was damaged by an earthquake in 2020. The present report includes the seismic assessment of the church thanks to numerical simulation and hand calculations, and propositions for the retrofitting of the structure.

The numerical simulation consists of static pushover analysis on a finite element model of the church performed on the software Abaqus. The approach for the modelling is the homogenised material model with 2D shell elements. Local failure mechanisms are also analysed through hand calculations. This seismic evaluation of the church, along with the observed damage on the church's structure, is the basis for the propositions of strengthening measures. Some retrofitting ideas are advanced and their adequacy in the case of this church is discussed, but no structural analysis of the retrofitted building is carried out.

Acknowledgments

First of all, I would like to thank the EESD laboratory at EPFL, and especially Prof. Katrin Beyer, Dr. Savvas Saloustros and Dr. Igor Tomic for giving me the opportunity to work on an interesting and stimulating project, and for providing me with great help and support throughout the process. The EESD laboratory also gave me the opportunity to spend a few days in Zagreb and visit the church in Petrinja, which I am very thankful for.

I also want to express my gratitude to the Faculty of Civil Engineering of the University of Zagreb, in particular Prof. Mario Uros who welcomed me and provided me with a working space while I was in Zagreb, and Dr. Maja Banicek for helping me with the numerical model. Her experience with Abaqus was crucial to the project. Finally I want to thank Martina Vujasinovic and her team for organizing the site visit and providing me with the necessary information about the church.

Contents

1 Introduction

Unreinforced masonry has always been one of the most common materials used for buildings all around the world, until the emergence of new materials like concrete and steel. These ancient masonry buildings were built without much static calculations, and the builders were relying mostly on their experience and rules of thumb to design buildings [2]. Seismic hazard was certainly not taken into account in the design back then, and unreinforced masonry is inherently vulnerable to earthquakes because of the low tensile strength of the mortar between the bricks. At the same time, these buildings are often complicated to analyse because of the large number of unknowns about the behaviour of masonry under dynamic actions, and because each building was built with the materials that were available in its surrounding area, so the material properties can vary a lot from one building to the other. Many of these historical masonry buildings are located in areas of high seismic activity like the Mediterranean Region, therefore one of the big challenges of seismic engineering is the preservation of these buildings of historical and cultural value.

One of these historical masonry buildings is the Kapela Sveti Nikola (figure 1), a chapel located in Petrinja, a Croatian town that was hit by an earthquake of magnitude 6.4 in December 2020. The church has suffered severe damage during this earthquake, with the collapse of the bell tower and many cracks in the whole structure. Therefore, a complete seismic assessment of the church is needed in order to then design the needed retrofitting interventions. The fact that this church was exposed to a strong earthquake recently allows to compare the results of the analysis with the actual performance of the church, which is very valuable for the interpretation of the results.

Figure 1: Kapela Sveti Nikola before the earthquake

This work is composed of two main parts : the first and biggest part is the seismic assessment of the building, while the second part addresses possible retrofitting solutions based on the results of the assessment and the observed damage. The seismic assessment is carried out with the help of a numerical simulation. Static pushover analysis is performed on a finite element model of the church to obtain the global capacity of the church, which is then compared to the demand thanks to the N2 method. The church is modelled with 2D shell elements and a homogenised material model, and the software used for the numerical simulation is Abaqus. Some local mechanisms are also analysed with hand calculations, following the procedure described by Godio & Beyer [10]. Based on the results of this seismic assessment and the visible damage on the church, some ideas for the retrofitting of the most critical parts of the church are proposed. Because it is a church with heritage value, the retrofitting measures should not only be effective in terms of the strengthening of the structure, but also respectful of the existing building. The minimal necessary intervention should always be favored over heavy intrusive measures, which is why a good assessment of the structure's resistance to earthquakes is necessary. The pros and cons of the proposed strengthening measures are discussed and the key aspects to take into consideration when implementing these measures are addressed, but the structural analysis of the retrofitted church is not part of this work.

The report is structured as follows. In section 2, the church is presented and the damage it suffered during the earthquake is reported. Section 3 presents the process for the estimation of the material properties. After that follows the report of the numerical simulation in section 4, with the modelling assumptions, the validation of the model thanks to simple tests, the methodology of the analysis and finally the results. Then, the hand calculations are presented in section 5. Section 6 addresses the retrofitting propositions, and finally section 7 discusses possibilities to improve the assessment and to go further in this project.

2 Presentation of the church

The Kapela Sveti Nikola is a small chapel located in a cemetery just outside of Petrinja, a town that lies in the County of Sisak-Moslavina, approximately 50 km southeast of the capital of Croatia, Zagreb (see figure 2).

Figure 2: Location of the church

The chapel is approximately 14 m long and 7 m wide and consists of a brick masonry structure with a timber roof. It is made of four walls that are approximately 5.5 m high, three of which are straight, while the apse wall is curved. These walls are linked together by a system of masonry arches and vaults : 5 double-curvature vaults that are approximately 20 cm thick rest on 4 arches which span in the transverse direction and are about 50 cm thick. Above these vauts lies the timber gable roof with its ridge at approximately 9 m of height. At the top of the southwest wall stands the rectangular bell tower made of brick masonry, supporting a timber spire. This tower is supported by the southwest facade and by two masonry columns located inside the chapel. The masonry tower reaches a height of approximately 13.5 m and the spire 18 m. The walls are relatively thick (between 0.5 m and 0.9 m). The church is almost symmetrical about the longitudinal axis, except for one side door in the southeast wall, and an opening on the northwest side of the bell tower. Figures 3 and 4 show the plan view of the ground floor and the longitudinal section.

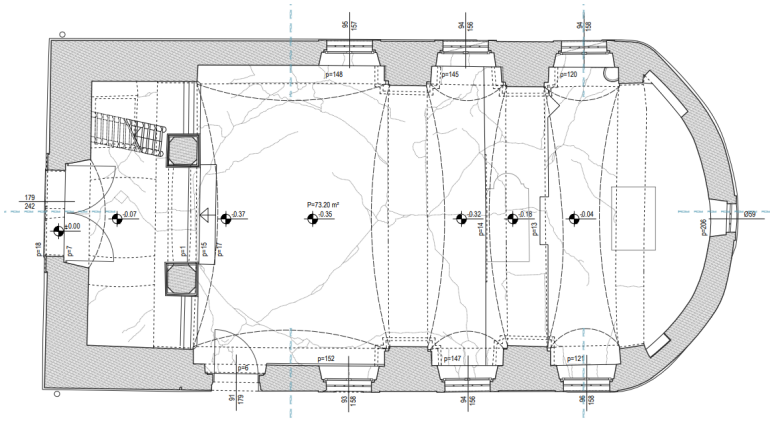

Figure 3: Plan view of the ground floor

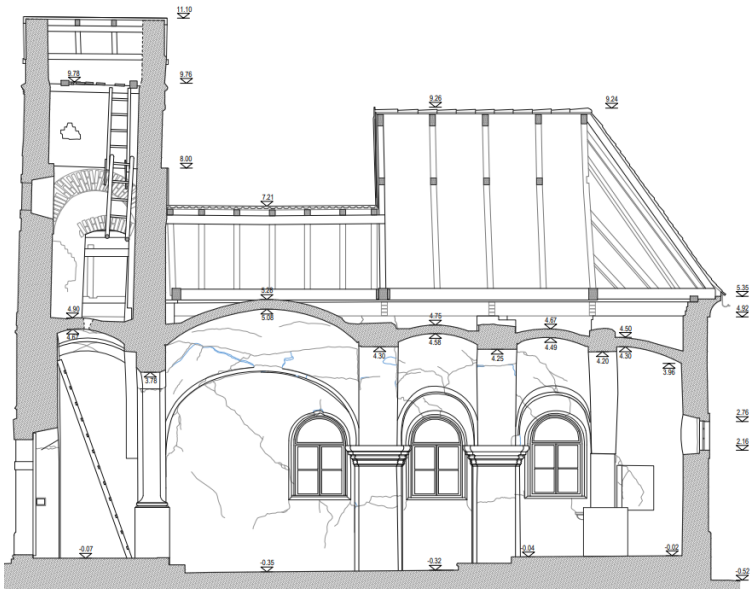

Figure 4: Longitudinal section

2.1 Earthquake and damage report

This church was struck by the earthquake of December 29^{th} 2020, whose epicentre was approximately 3 km to the southwest of Petrinja. The earthquake was felt in most of the northern part of Croatia, and even in neighbouring countries such as Bosnia and Slovenia. With a magnitude of 6.4 on Richter's scale and a depth of 10 km [7], it was the strongest earthquake in Croatia since 1942 [15]. Many buildings in Petrinja, as well as in other villages and towns in the surroundings, were destructed or heavily damaged. The highest observed intensity was between XVIII (heavily damaging) and IX (destructing) on the European macroseismic scale [19]. There were many aftershocks in the hours following the main earthquake, with magnitudes up to 4.9.

The most obvious damage was the failure of the bell tower, where the spire and the top part of the masonry tower completely fell of (see figure 5). It fell on the timber roof which was largely destructed. The vaults show some huge cracks, due partly to the seismic forces and partly because the bell tower fell on them. We can also see many cracks in all the walls, with the plaster coming off in some places.

Figure 5: Condition of the church after the earthquake

The part of the roof that was destructed has now been temporarily repaired with a metal sheet covering. The bell tower has also been covered. This is to avoid further damage on the inside due to the rain. There are also some temporary braces on the inside to give the vaults and walls additional support.

The church in its current state is very well documented. There are blueprints of all the facades, plan views and sections where the cracks are reported which really helps the identification of failure mechanisms. The blueprints, as well as some photos, were provided by Martina Vujasinovic. However, there is not much documentation about the church before the earthquake, so some dimensions (e.g. height of the bell tower, weight of the spire) had to be roughly estimated based on photos.

For the rest of the report and for the calculations, the longitudinal axis of the church will be referred to as the X axis (NE-SW direction), the transverse axis as the Y axis (NW-SE direction) and the vertical axis as the Z axis (see figure 6).

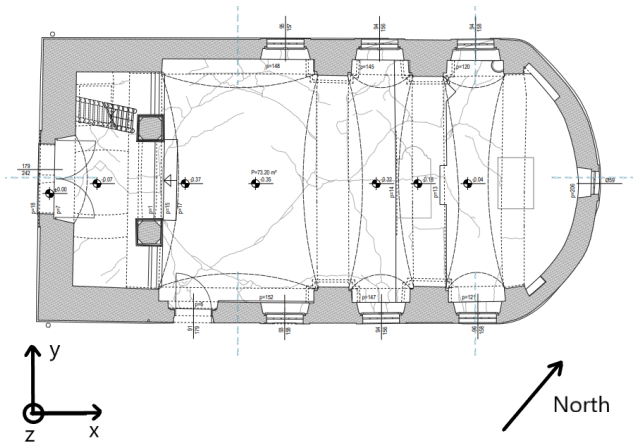

Figure 6: Coordinate system and direction of the North

3 Material properties

The estimation of the properties of the masonry is a difficult task, since there are many parameters that can have a big influence on these properties, such as the quality of the bricks, the quality of the mortar, the layout of the bricks and the conservation of the materials [12]. Furthermore, no tests have been carried out on the materials of the Kapela Sveti Nikola. Therefore, the properties have to be estimated based on tests carried out on similar masonry elements and empirical relations or values found in literature.

The masonry will be modelled as a homogenised, isotropic material, so the properties needed for the analysis are not the properties of the bricks and the mortar, but the general properties of the unreinforced masonry material. Many different material models are available in Abaqus, and the Concrete Damaged Plasticity model is chosen, which is usually used for modelling masonry as a homogenised material. The properties needed for a static analysis in Abaqus with this model are the following :

- Density (γ)
- Young's modulus (E)
- Poisson's ratio (ν)
- Stress - strain relation in compression
- Tensile behaviour (can be defined in different ways)

A few additional parameters have to be specified for the Concrete Damaged Plasticity model : dilation angle, eccentricity, f_{b0}/f_{c0}, K and a viscosity parameter.

First, the components of the masonry that were used in the church have to be identified. The bricks are made of clay and are solid, and the dimensions appear to be approximately 280 by 130 by 65 mm, with quite a high variability. The mortar is probably lime-based, since most of the ancient buildings of this area are built with this type of mortar.

For the compressive strength, Maja Banicek recommended a Croatian book [23] which used a value of 3.4 MPa for the analysis of a typical building in Zagreb with a similar type of masonry. This value is also in the range of values suggested by the Italian standards (Table C8.5.1) [3], which is 2.6-4.3 MPa.

The tensile strength of the masonry is estimated based on the European database on masonry wall tests [9]. In this database, the tests that were carried out on similar masonry typologies as the one in the church are selected. The selection criteria are the following : solid clay bricks with the same dimensions $+/-$ 10 %, pure lime mortar or mostly lime with a small proportion of cement mortar. The average value of tensile strength is calculated on the 30 selected data entries (tests n° 5-8, 80-94, 99-105 and 212-215).

For the estimation of the Young's modulus of masonry, many empirical relations exist, most

of which are a linear relation between the Young's modulus and the compressive strength. SIA 266 [20] for example gives the following formula :

$$E = 1000 \cdot f_c \tag{1}$$

But this has been shown to be an over-estimation of the stiffness by many studies, especially for old masonry. More conservative relations can be found in literature, and the relation given by Kaushik et al. [12] will be used.

$$E = 550 \cdot f_c \tag{2}$$

Since this equation gives a value (1870 MPa) that is larger than the maximum value given by the Italian standards, the maximum value of 1800 MPa will be used. The basic material parameters are presented in Table 1.

Property	**Value**	**Unit**	**Source**
γ	18	kN/m^3	[21]
ν	0.2	-	[13]
f_c	3.4	MPa	[23]
f_t	0.15	MPa	[9]
E	1800	MPa	[3]

Table 1: Material properties

To define the stress - strain curve in compression, the control points given by Kaushik et al. [12] are used. The resulting stress - strain curve is shown in figure 7.

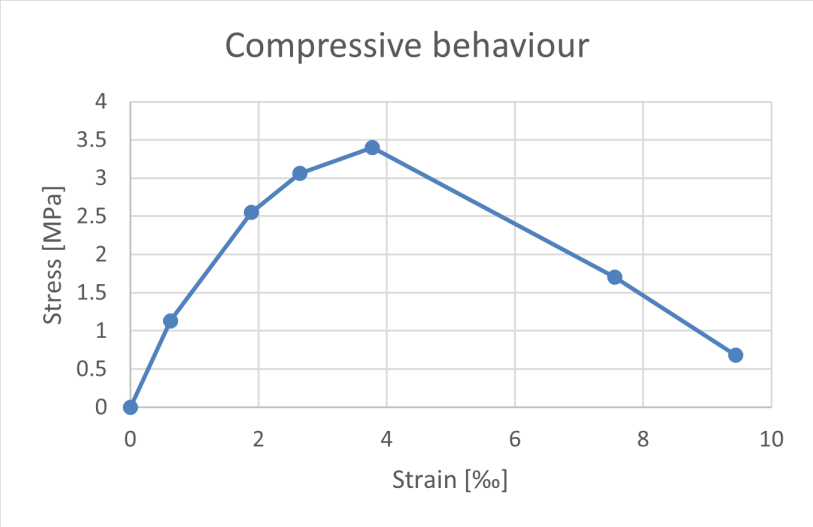

Figure 7: Stress - strain curve of the masonry in compression

To define the post-failure behaviour in tension, three options are available in the Concrete Damaged Plasticity material model : stress in terms of strain, stress in terms of displacement, and the definition of the fracture energy. Lourenço & Gaetani [13] recommend a value of

fracture energy of 0.02 N/mm in tension. But it is important to note that in Abaqus, the residual tensile strength has to be set to a non-zero value to avoid convergence problems, which is not possible with the definition of the fracture energy. So the option that was chosen is to define the stress in terms of displacement, with a residual strength of 0.01 MPa and a corresponding displacement that gives a fracture energy of 0.02 N/mm.

For the additional parameters required by the Concrete Damaged Plasticity model that were mentioned above, the default values are used, except for the viscosity parameter which has an important influence on the results. This parameter is a fictive viscosity that helps to achieve convergence by overcoming local instabilities, but a value that is to high can lead to inaccurate results. So a small sensitivity analysis was done to see in which range of values the results seem stable and consistent with each other. The default value is 0, but with this value convergence problems appeared. With values higher than $5 \cdot 10^{-4}$, the force capacity tends to be overestimated. In the range of 10^{-5} to $5 \cdot 10^{-4}$, the analyses converge and the results are consistent, with differences in the force capacity in the order of 1 %. The value that is chosen for the analysis of the church is the smallest one in the range above, so that overestimation of the force capacity can be avoided as much as possible. The values used for these parameters are presented in table 2.

Dilation angle	Eccentricity	f_{b0}/f_{c0}	K	Viscosity parameter
34°	0.1	1.16	0.67	10^{-5}

Table 2: Additional parameters for Concrete Damaged Plasticity model

4 Numerical simulation

In order to estimate the capacity of an existing unreinforced masonry building to resist to earthquakes, a nonlinear analysis is usually necessary. Many different approaches are possible for the modelling of the structure [1].

- Micro-model, where bricks/stones and mortar are modelled explicitly
- Homogenised material model, where the structure is modelled with an average masonry material
- Macro-element model, where the structure is modelled with macro-elements (piers and spandrels)

The micro-modelling approach is computationally too expensive for the level of precision required in this type of analysis, and is more suited for single strucural elements rather than a whole building. The macro-element modelling approach is the least expensive in terms of computational cost, and is well suited for regular buildings, where all the stories are pretty similar, and the openings are aligned with each other. However, it is not adapted to less regular buildings like churches. The choice for this analysis is therefore the homogenised material approach. Then, two different analysis procedures are possible : static pushover analysis, where a monotonic load is applied in small increments to simulate the seismic forces, and dynamic time-history analysis, where a ground motion (an accelerogram) is applied to the structure and its response is calculated. The static pushover analysis is chosen, again for computational cost reasons.

The software that was chosen to run this analysis is Abaqus, a program that is well-suited and often used for nonlinear analysis of structures. The choice was made to create a shell model with 2D elements instead of a solid model with 3D elements, in order to reduce the computational cost of the analysis. The downside is a possible slight loss in accuracy, especially in the out-of-plane (OOP) behaviour of walls. Every masonry section of the church (wall, vault, column, etc) is replaced in the model by a shell section representing its middle surface. A homogenised, isotropic material as well as a thickness is assigned to every shell section.

4.1 Modelling assumptions

In order to model a building with a relatively complex geometry like a church with a shell model, some assumptions and simplifications are needed. The goal is to produce a model that is not too complicated, with a valid geometry where all parts of the church are connected together as they should, and that can be meshed without requiring too many finite elements.

4.1.1 Geometry and Boundary conditions

First, the church is considered fixed on the ground, and the foundation is not modelled. The reason is that no information is available on the foundation of the church, and this assumption

is usually sufficient for a pushover analysis of a structure.

Another assumption is that the middle surface of adjacent walls are considered to be aligned with each other, which means that the potential offsets between the middle surfaces of walls (due to a change of thickness) is not considered (see example in figure 8). This is done to represent the interaction between adjacent walls as close to reality as possible. Indeed, if the offsets were modelled, the displacement of the walls would have to be constrained, for example with Multi-Point Constraints (MPC), which would be unnecessarily complicated.

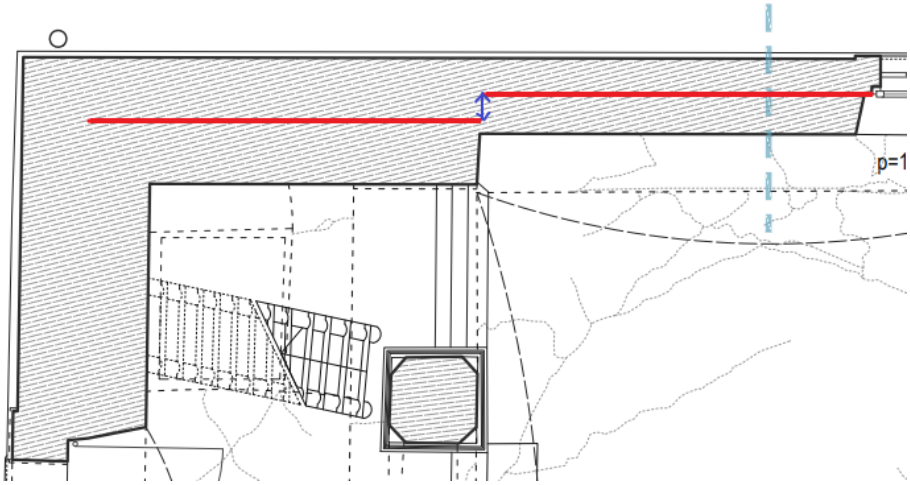

Figure 8: Example of simplification for the offset between walls. Red : middle surfaces of the two adjacent walls. Blue : offset between the middle surfaces that is neglected in the model

The arches above the windows and main door are not modelled, the shapes of these openings are simplified to rectangles. This allows a simpler and more regular mesh without changing the behaviour too much. The small round windows of the southwest facade and the apse are completely ignored (see example in figure 9).

(a) Southwest facade

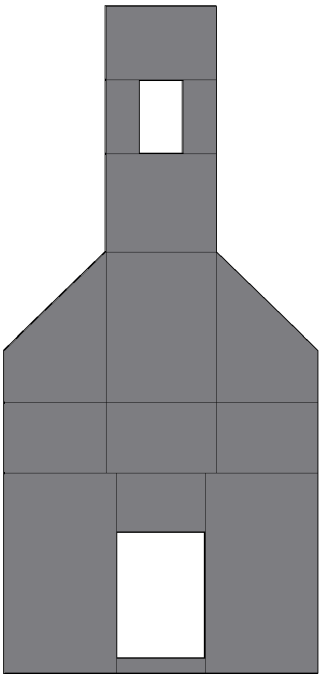

(b) Model of the southwest facade

Figure 9: Example of simplification of the openings. The window and the door are modelled with a rectangle, and the small round windows are ignored.

Another simplification that needs to be done is to replace the curved apse with three straight segments of wall (see figure 10). Indeed, when importing the geometry into Abaqus, the link between the curved apse and the adjacent vault generated some invalid geometry. But with the apse represented with three straight segments, this problem disappears, and the influence on the results should not be to big.

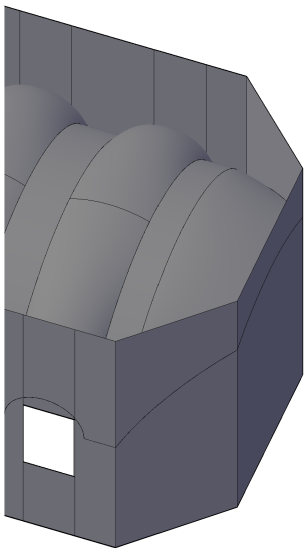

Figure 10: Modelling of the apse with 3 straight segments

The geometry of the vault that is directly under the bell tower also has to be simplified in order to obtain a valid geometry. From the blueprints, it seems to be a double-curvature vault, but in the model it was replaced by a barrel vault spanning in the Y axis, so as to avoid problems in the link between the vault and the bell tower above.

As the church is quite old, the geometry is not completely regular : some walls are slightly inclined, the thickness of the elements varies a little bit, there are some misalignments, etc. These aspects are all ignored in the model. As for the thickness, different elements that have a similar, but not exactly identical thickness are assigned the same thickness in the model. This means that a wall could be slightly thicker or thinner in the model than it is in reality. Six different section thicknesses are defined in the model, and every part of the church is assigned one of these six thicknesses according to the dimensions found in the blueprints of the church (see figure 11).

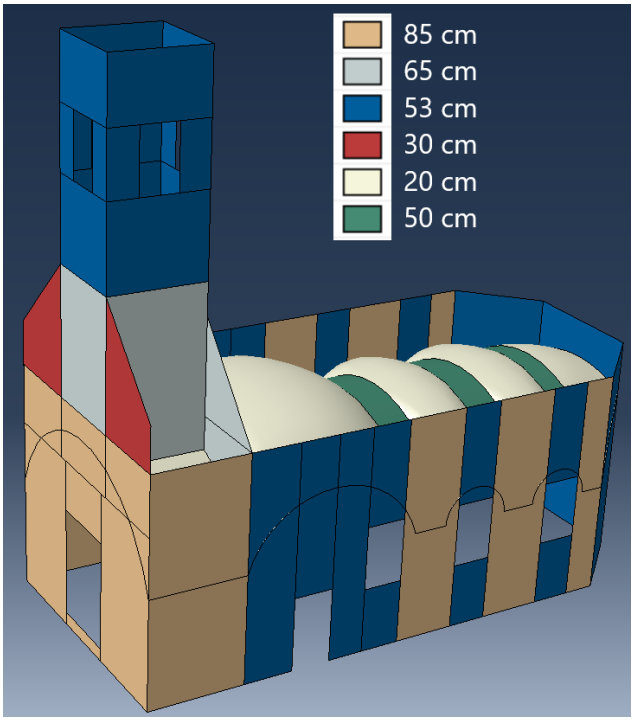

Figure 11: Thickness assignments to the different parts of the church

4.1.2 Roof and spire

Only the masonry structure is modelled. Indeed, the timber roof is very flexible compared to the masonry, and is probably only transmitting vertical loads to the masonry walls since the timber structure forms a closed triangle. Therefore, the horizontal stiffness of the roof structure is negligible compared to the masonry structure. Based on this assumption, only the mass of the roof has to be added to the model. The mass of the roof is estimated based on the dimensions and spacing of the timber beams and the area of tiles covering that can be seen on the blueprints of the church. A density of 500 kg/m^3 for the wood and a mass per unit area of 75 kg/m^2 for the tiles has been assumed (SIA 261 Annex A [21]). The roof mass

is applied as lumped masses on the top edge of the walls. Based on the assuptions mentioned above, it was estimated to 600 kg/m of wall, which is then multiplied by the average spacing between the nodes at the top edge of the walls to find the mass that has to be applied to each node.

The same has to be done for the mass of the spire at the top of the bell tower, except that there are no blueprints showing the spire structure, so the estimation is based on photos from before the earthquake and is very rough. The total mass of the spire is assumed to be 2000 kg, which is applied on the bell tower in the same way as the roof load. The nodes on which the roof and spire masses are applied are displayed in figure 12.

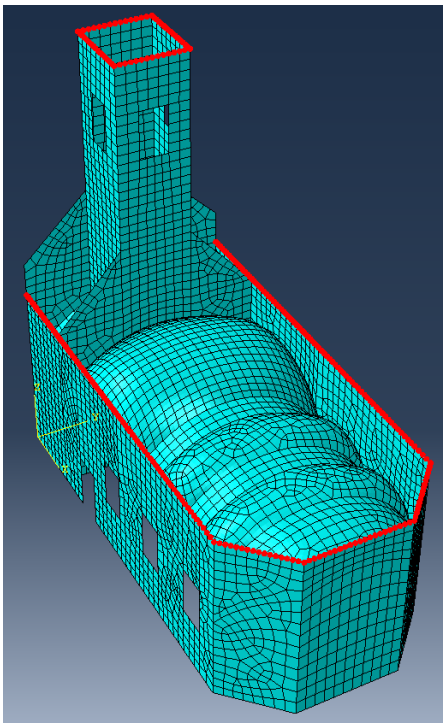

Figure 12: Points of application of the lumped masses of the roof and spire (in red)

4.1.3 Mesh

The meshing for a Finite element model is a complicated task, since there are many choices that have to be made and all of them can have an important influence on the results of the analysis [18]. One has to choose the type of element (triangle, quadrilateral, etc.), the order of the interpolation functions, the integration rule and number of integration points through the thickness, as well as the size of the elements.

The main concern when using shell elements is to capture the OOP behavior correctly. Zsofia Salat's thesis [18] investigated the influence of meshing choices on the OOP behavior of walls, and the results of the first example, which has similar characteristics as the members found in the church, suggest the following : quadrilateral elements with quadratic interpolation (8 nodes per element) and with 9-point Simpson integration through the thickness give accurate

results, and the results stay relatively consistent with mesh refinement.

The meshing options for the church are chosen accordingly, with mostly quadrilateral elements and few triangular ones were the geometry requires it. The target element size is set to 300 mm, and then the mesh is generated automatically on Abaqus. This size choice allows a mesh where the element size is quite constant in the whole model, and the total number of elements (5164) is low enough to keep an acceptable computational cost. Abaqus can perform a mesh verification which resulted in no invalid elements, although there are warnings for a limited number of elements (less than 4 %), which are highlighted in figure 13. These elements are either distorted or curved/warped, and are located mostly in the corners of the vaults, where the curvature is larger.

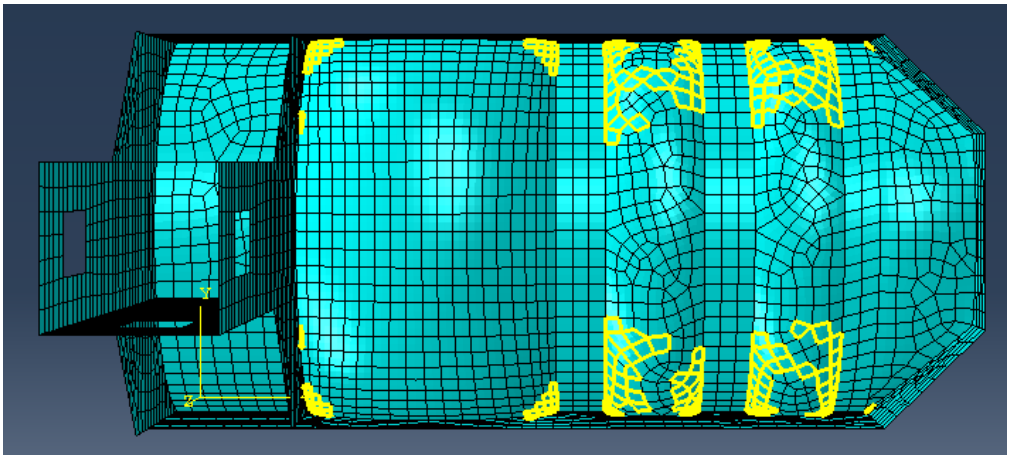

Figure 13: Element warnings in the vaults (in yellow)

4.2 Validation of the model

Because the verification of the results of the pushover analysis of the whole church is difficult, tests should be performed on simple wall models first, for which the verification of the result is possible thanks to hand calculations.

The goal of this validation of the model is to simulate three different failure modes of masonry walls that could be observed in the church : in-plane rocking mechanism, in-plane diagonal shear mechanism and out-of-plane mechanism. For all three, some values from the analysis can be compared to hand calculations with formulas from codes or literature : for the in-plane mechanisms, the initial stiffness and the peak load of the pushover curve can be verified ; for the OOP mechanism, the pushover curve can be compared to the force-displacement response of the rocking movement of a rigid body. The dimensions of the tested walls are similar to the walls of the church, so that the mesh size used in the tests can also be used in the church model.

4.2.1 In-plane rocking mechanism

Rocking is the predominant failure mechanism for slender cantilever walls. The wall that is chosen to test this mechanism is a segment of wall in between two windows in the southeast or northwest facade. Its dimensions are the following :

- Height : $h = 5500$ mm
- Length : $l = 1470$ mm
- Thickness : $t = 850$ mm

The tested system is a cantilever wall with a constant uniform axial load applied at the top, and a concentrated lateral force at the top which is incremented during the analysis (see figure 14). The axial load is set to 400 N/mm, which corresponds to an axial stress of 0.47 MPa and an axial load ratio of 13.8 %.

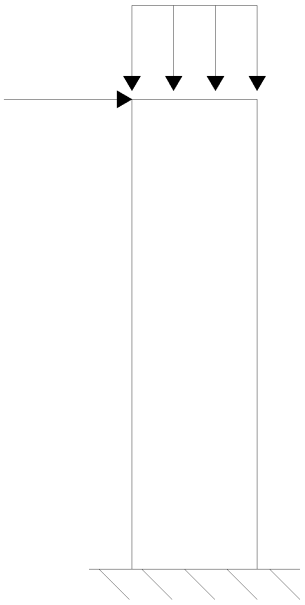

Figure 14: Sketch of the analysed system for the in-plane rocking mechanism

The expected initial stiffness K_{ini} can be calculated with the combination of the flexural stiffness K_b and the shear stiffness K_s :

$$K_{ini} = \frac{1}{\frac{1}{K_b} + \frac{1}{K_s}} \tag{3}$$

With :

$$K_b = \frac{3EI}{h^3} = \frac{3E \cdot \frac{t \cdot l^3}{12}}{h^3} \tag{4}$$

$$K_s = \frac{GA}{h} = \frac{\frac{E}{2(1+\nu)} \cdot l \cdot t}{h} \tag{5}$$

The rocking resistance of a masonry wall can be calculated with the simplified equation from EC8 part 3, Annex C [6] :

$$V_{Rd,R} = \frac{l \cdot N_x}{2h} \cdot \left(1 - 1.15 \frac{N_x}{l \cdot t \cdot f_c}\right) \tag{6}$$

It can be checked that rocking is indeed the critical mechanism by computing the diagonal shear resistance as well, with the equation from Tomazevic [22] :

$$V_{Rd,S} = \frac{l \cdot t \cdot f_t}{b} \cdot \sqrt{\frac{N_x}{l \cdot t \cdot f_t} + 1} \tag{7}$$

With b the shear stress distribution factor, which can be assumed to be 1.5 for $h/l \geq 1.5$ [22].

The wall is then modelled in Abaqus with a planar section, which is meshed in the same way as the church model (more detail on the mesh is given in Section 4.1.3). The analysis is then performed in two steps : in the first step the axial load is applied, and in the second step the lateral load is applied with an arc-length controlled incrementation, until the top displacement reaches 100 mm. To avoid stress concentration at the point of application of the load, a Multi-Point-Constraint is added to constrain the lateral displacement of all the nodes on the top edge of the wall. The geometric non-linearity is accounted for in all the analyses.

The distribution of plastic strains on the wall (figure 15) confirms a rocking failure, with tensile failure at the bottom left corner. The force-displacement curve (total base shear over displacement of the top of the wall) can then be plotted (figure 16), and the values of interest (initial stiffness and ultimate load) can be read on the graph and compared to the values calculated by hand (table 3).

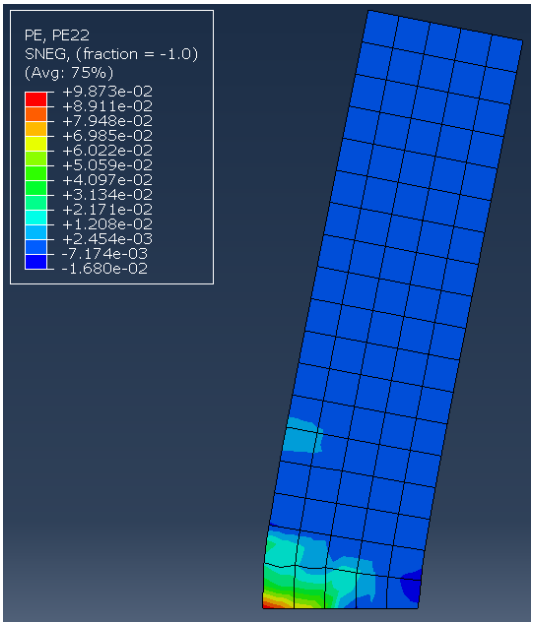

Figure 15: Distribution of vertical plastic strains in the slender wall at a top displacement of 100 mm

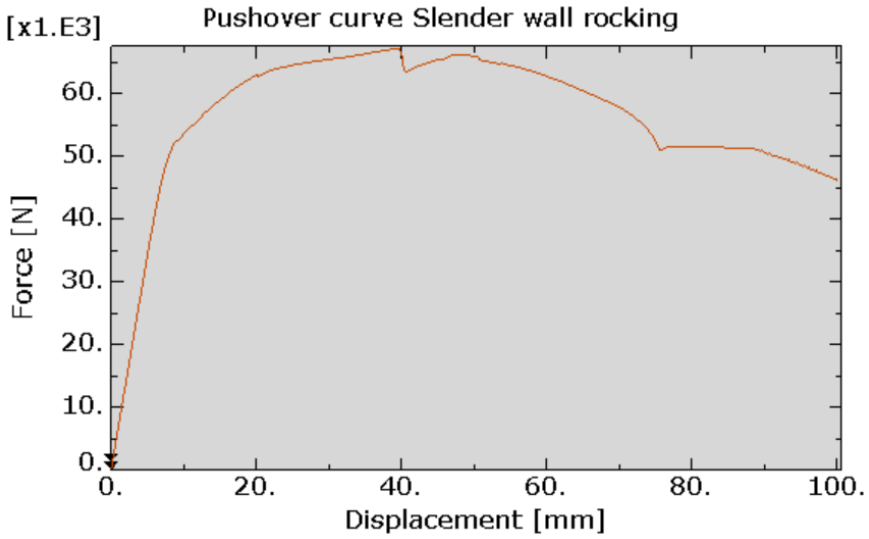

Figure 16: In-plane pushover curve of the slender wall

Quantity	Hand calculation	Abaqus	Difference
K_{ini}	7.00 kN/mm	6.84 kN/mm	2.3 %
$V_{Rd,R}$ $V_{Rd,S}$	**66.1 kN** 254.2 kN	67.1 kN	1.5 %

Table 3: Comparison of hand calculations and Abaqus results for in-plane rocking mechanism

The hand calculations and the finite element analysis show very similar results for the initial stiffness and for the ultimate load. The failure mechanism is the expected one, so this confirms that the in-plane rocking mechanism is captured correctly in the finite element analysis.

4.2.2 In-plane diagonal shear mechanism

To produce a diagonal shear failure instead of a rocking failure, the cantilever wall should be less slender. The length of the wall that is considered is from the corner of the church to the window in the northwest facade. The considered height is half the height of the wall, so that the tested wall is really squat and the shear mechanism is critical. Its dimensions are the following :

- Height : $h = 2750$ mm
- Length : $l = 5310$ mm
- Thickness : $t = 850$ mm

The tested system, which is sketched in figure 17, and the axial load are the same as for the slender wall.

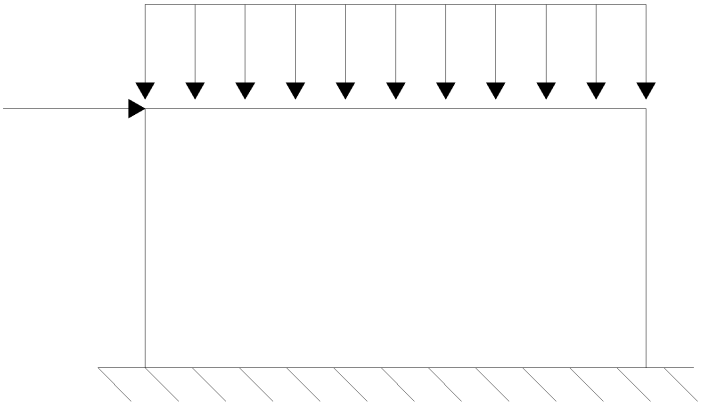

Figure 17: Sketch of the analysed system for the in-plane diagonal shear mechanism

The expected initial stiffness and the rocking and diagonal shear resistance are computed in the same way as for the slender wall. For the diagonal shear resistance, the shear stress distribution factor b can be assumed to be 1 for $h/l \leq 1$ [22].

After performing the analysis similarly to the slender wall until a top displacement of 10 mm, the plastic strain distribution shows the formation of a diagonal shear crack (figure 18). Figure 19 displays the force-displacement curve and the comparison of the hand calculations and Abaqus results is presented in table 4.

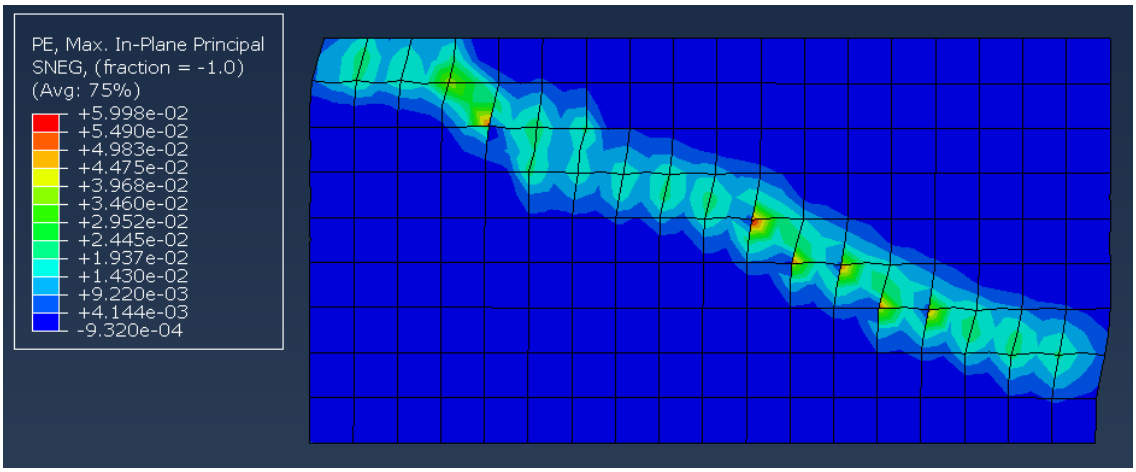

Figure 18: Distribution of maximal principal plastic strains in the squat wall at a top displacement of 10 mm

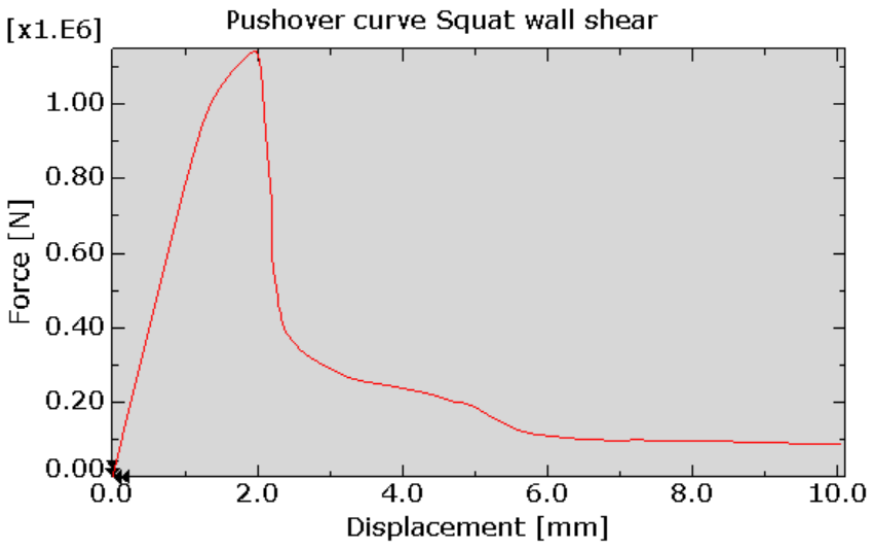

Figure 19: In-plane pushover curve of the squat wall

Quantity	Hand calculation	Abaqus	Difference
K_{ini}	851 kN/mm	788 kN/mm	7.4 %
$V_{Rd,R}$ $V_{Rd,S}$	1724 kN **1377 kN**	1142 kN	17 %

Table 4: Comparison of hand calculations and Abaqus results for in-plane shear mechanism

The difference between the results of the hand calculations and the Abaqus analysis are a bit larger for the shear failure, compared to the rocking failure. But it has to be noted that the shear resistance of unreinforced masonry is known to be harder to predict, and the result of equation (7) is not necessarily perfectly accurate. However, the observed failure mechanism as well as the comparison show that the results of the finite element analysis are not too far from the reality. It is interesting to note as well that the shear mechanism is much more brittle than the rocking mechanism, with the load dropping very quickly to a small value after the peak. The displacement capacity is much smaller for shear than for rocking, which is expected.

4.2.3 Out-of-plane mechanism

The OOP response is tested on the same wall as the in-plane rocking, but with an OOP loading. The axial load is still 400 N/mm. A uniform linear lateral load is applied on the whole top edge of the wall, and incremented during the analysis.

The pushover curve obtained in Abaqus can be compared to the force-displacement response of a rocking rigid body. The tensile strength is neglected and the compressive strength is considered infinite. With these assumptions the moment equilibrium can be formulated:

$$\sum M = F \cdot h - N_x \cdot \left(\frac{t}{2} - \delta\right) = 0 \tag{8}$$

Based on this, the force F_0 needed to onset the mechanism can be calculated by stating $\delta = 0$:

$$F_0 = \frac{N_x \cdot t}{2 \cdot h} = 45.4\,kN \tag{9}$$

The displacement δ_0 at which the lateral load capacity drops to zero can be calculated by stating $F = 0$:

$$\delta_0 = \frac{t}{2} = 425\,mm \tag{10}$$

With these two parameters, the linear capacity curve can be plotted on the same graph as the pushover curve generated with Abaqus (figure 20).

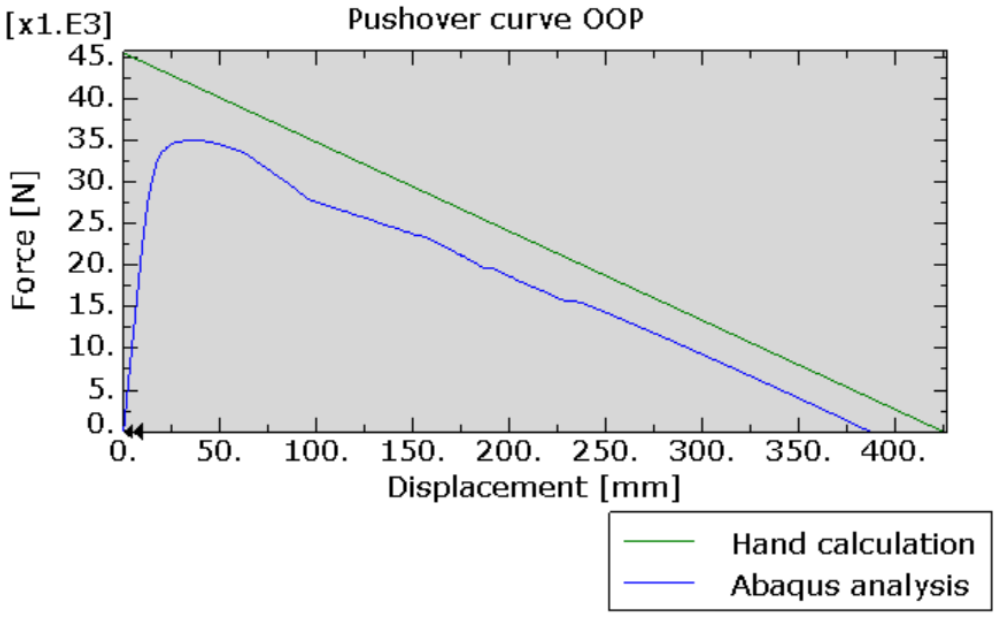

Figure 20: Out-of-plane pushover curve of the slender wall

The comparison of the two curves shows that the OOP behaviour is described correctly in Abaqus. The force capacity is a bit lower than with the hand calculation, but this is normal since the compression strength was considered infinite in the hand calculations. The fact that the slopes of the two curves are very similar after the peak shows that the geometric non-linearity (P-Δ effect) is captured as it should.

4.3 Methodology

Once the church is modelled and meshed in Abaqus, the first thing that can be done is a modal analysis. The extraction of the eigenvectors, along with the other modal parameters like the modal frequencies, the participation factors, the modal masses and the effective modal masses is useful for different reasons. First it allows to check that the model behaves correctly, and the modal parameters are also needed for the comparison of the capacity of the structure with the demand, because the Multiple-degree-of-freedom (MDOF) system has to be transformed into a Single-degree-of-freedom (SDOF) system. The first 50 modes are

extracted. For the modal analysis, only the elastic material properties are needed (E, ν and γ).

Then, the nonlinear pushover analyses can be carried out in three different directions :

- $+$X : longitudinal direction, pushing the bell tower towards the rest of the church
- $-$X : longitudinal direction, pushing the bell tower away from the rest of the church
- $+$Y : transverse direction, towards the northwest

Since the church is almost symmetrical about the X axis, the pushover analysis in the $-$Y direction is not carried out, because the results would be really close to the $+$Y direction. Similarly to the tests on simple walls described in section 4.2, the analysis is done in two consecutive steps : first the gravity loads are applied (self weight of the masonry and weight of the roof and spire), and then the lateral load is applied with an arc-length controlled incrementation. The lateral load is applied as a mass-proportional body force on the whole model. The geometric non-linearity is accounted for.

After running the analysis, the first thing to do is to look at the deformed shape and damage pattern, and check if it corresponds to what is expected and to the damage that was actually observed on the church. Then, the pushover curve can be computed in each direction by plotting the total base shear V_b over the displacement of the reference node δ_{ref}, which is the node that has the biggest displacement in the whole model.

Then, in order to compare the capacity that is determined by the pushover curve to the demand, the N2 method [8] is used. The principle of this method is to plot in a same graph the pushover curve of the structure (in acceleration-displacement format), which represents the capacity, and the Acceleration-Displacement Response Spectrum (ADRS), which represents the demand. The performance point of the structure is found at the intersection of the capacity and the demand curve.

The ADRS is a combination of the acceleration response spectrum and the displacement response spectrum, based on the elastic response spectrum that can be found in different seismic codes (SIA 261 [21] is used), and depends on the peak ground acceleration and soil class at the location of the structure. The peak ground acceleration a_{gd} for a return period of 475 years at the location of the church can be found on an online map from the Department of Geophysics of the University of Zagreb [11]. There is not much information about the soil parameters at the location of the church, but according to Igor Tomic, the important damage suffered by many buildings in the area of Petrinja during the 2020 earthquake could be explained partially by a low quality soil, which amplifies the acceleration response of buildings. Based on this information, the soil is assumed to be of Class D. The parameters used for the computation of the Response spectrum are presented in table 5.

Soil class	S	T_B	T_C	T_D	a_{gd}
D	1.7	0.1 s	0.5 s	2 s	0.151 g

Table 5: Seismic data for the location of the church

Based on these parameters, the elastic acceleration response spectrum S_{pa} is defined, by assuming a damping of 5%. Then, the elastic displacement spectrum S_u is calculated with the following relation :

$$S_u = \frac{S_{pa}}{\omega^2} \tag{11}$$

With :

$$\omega = \frac{2\pi}{T} \tag{12}$$

Finally, the acceleration spectrum is plotted over the displacement spectrum to get the ADRS.

Since the response spectrum is defined for a SDOF system, the pushover curve of the structure (which is a MDOF system) has to be transformed into a capacity curve of an equivalent SDOF system in order to compare the capacity with the demand. But first, the pushover curve is approximated with a bilinear capacity curve, so that the comparison is more convenient [1]. Three quantities are needed to define the bilinear curve :

- Effective stiffness, taken as the secant stiffness at 70 % of the ultimate strength
- Ultimate strength
- Displacement capacity, taken as the displacement at 80 % of the ultimate strength in the post-peak region

Then, the acceleration capacity a^* of the equivalent SDOF system is obtained by dividing the base shear of the MDOF system by the effective mass of the most participating mode m_{eff}, i.e. the mode with the largest effective mass. In a regular building, this is usually the first mode, but in a church with an irregular geometry, it can be a higher mode.

$$a^* = \frac{V_b}{m_{eff}} \tag{13}$$

The displacement of the equivalent SDOF system is obtained by dividing the displacement of the reference node by the modal participation factor Γ and by the displacement of the reference node in the mode shape a_{ref}.

$$\delta^* = \frac{\delta_{ref}}{\Gamma \cdot a_{ref}} \tag{14}$$

Then, the capacity and demand curves can be plotted on the same graph and the results interpreted. If the capacity curve intersects the ADRS in the elastic region, the performance point of the structure is at the intersection and it means that the structure remains elastic

(the force capacity is not exceeded). However, if the capacity and demand do not intersect, the force capacity is exceeded and the displacement demand has to be calculated according to Eurocode 8 - part 1 [5] in order to perform a displacement-based verification.

The displacement demand depends on the period of the SDOF system T^*, which can be computed with equation (12), since the slope of the linear part of the pushover curve is equal to ω^2. If the period is larger than T_C, the equal displacement rule applies, which means that the displacement demand of the inelastic system is equal to the displacement demand of the equivalent elastic system. Therefore, the displacement demand is found at the intersection of the elastic capacity curve with the ADRS.

However, if the period is smaller than T_C, the equal displacement rule does not apply and the displacement demand δ_d^* is computed from the displacement demand of the elastic system δ_{el}^* as follows :

$$\delta_d^* = \frac{\delta_{el}^*}{q_u} \cdot \left(1 + (q_u - 1)\frac{T_C}{T^*}\right) \tag{15}$$

With :

$$q_u = \max\left(\frac{S_{pa}(T^*)}{a_{ult}^*}; 1\right) \tag{16}$$

Finally, it can be verified that the displacement capacity is larger than the displacement demand, and the performance point is considered to be at the displacement demand and the acceleration capacity of the system.

4.4 Results

4.4.1 Modal analysis

The parameters for the modes whose effective mass in one of the two main directions is more than 10 % of the total mass (416.8 ton) of the church are presented in table 6. Figures 21 and 22 show the deformed shapes of these modes. The other modes do not contribute as much in the seismic response of the structure. The participation factors depend on the normalization of the eigenvectors, and Abaqus automatically performs a mass normalization, which means that the amplitude of the eigenvectors are such that the modal mass (called "generalized mass" in Abaqus) is equal to 1.

Mode number	T [s]	Γ_X [mm^{-1}]	Γ_Y [mm^{-1}]	$m_{eff,X}$ [t]	$m_{eff,Y}$ [t]
1	0.23	9.48	0.169	89.8	0.029
2	0.17	0.212	-14.1	0.045	197.5
3	0.13	0.115	8.92	0.013	79.5
6	0.08	-12.7	-0.441	161.7	0.19
11	0.06	-7.39	0.863	54.6	0.74

Table 6: Modal parameters of the most participating modes

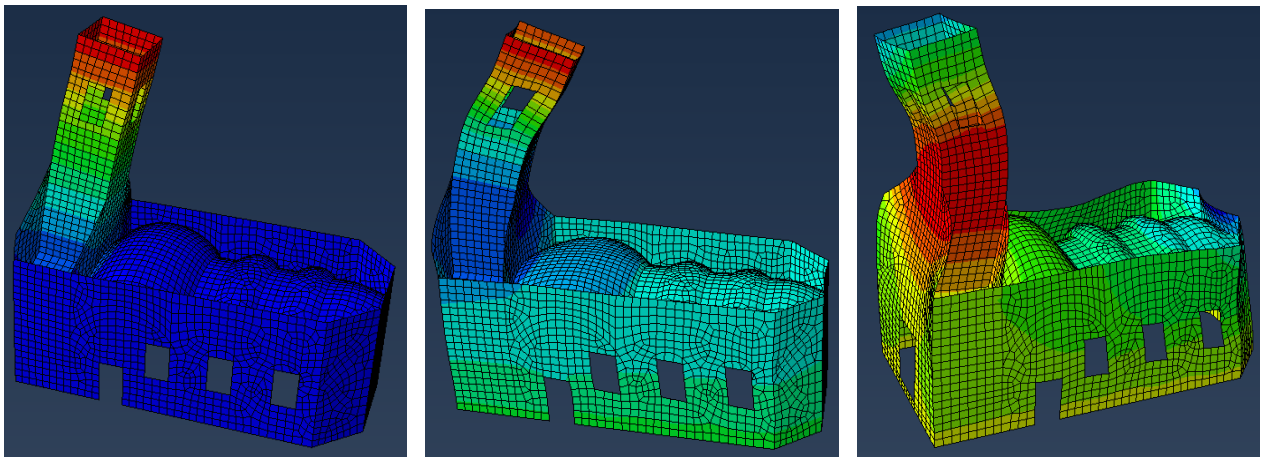

(a) Mode 1 **(b)** Mode 6 **(c)** Mode 11

Figure 21: Mode shapes of the 3 most participating modes in the X direction

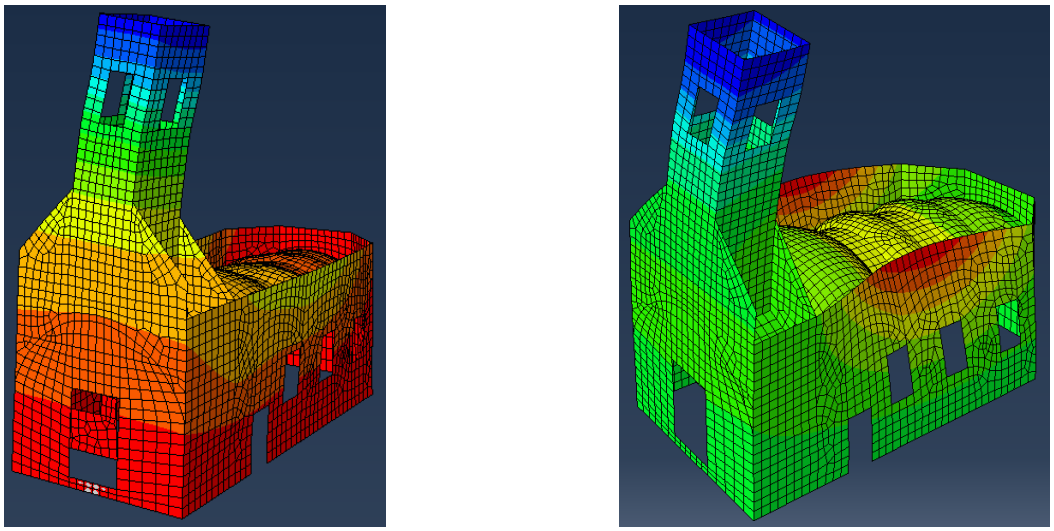

(a) Mode 2 **(b)** Mode 3

Figure 22: Mode shapes of the 2 most participating modes in the Y direction

This modal analysis shows that the model behaves as expected. The mode shapes make sense, as in the first mode of each direction all the nodes move in the same direction, and in higher modes some parts of the church move one way and other parts move the other way. The natural periods are also in a range that is expected for this type of building. The sum of the effective masses in each direction converges to the total mass of the building, which also indicates that the modal analysis is correct.

It is interesting to note that in the X direction, it is not the first mode that has the highest effective mass. This can be explained by the irregular shape of the church. Indeed, in the first mode, only the bell tower is moving, which leads to a relatively low effective mass compared to what could be expected for the fundamental mode. The modes that are used for the transformation from the MDOF system to the SDOF system are the ones with the largest

effective mass in each direction, i.e. mode 6 in the +X and −X directions, and mode 2 in the +Y direction.

4.4.2 Pushover analysis in +X direction

After running the pushover analysis, it is possible to look at the deformed shape of the church (figure 23), and also the distribution of plastic strains (figure 24) to identify the failure mechanism.

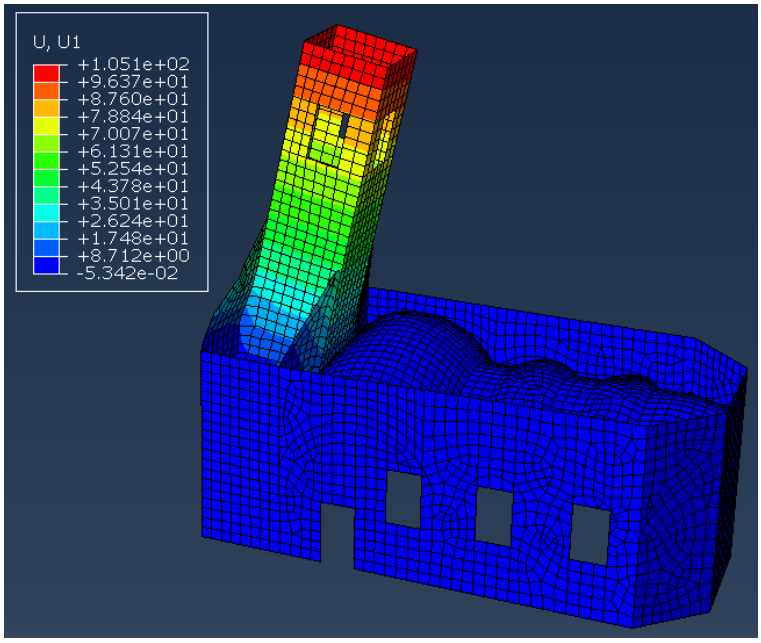

Figure 23: Displacement distribution for the pushover analysis in the +X direction

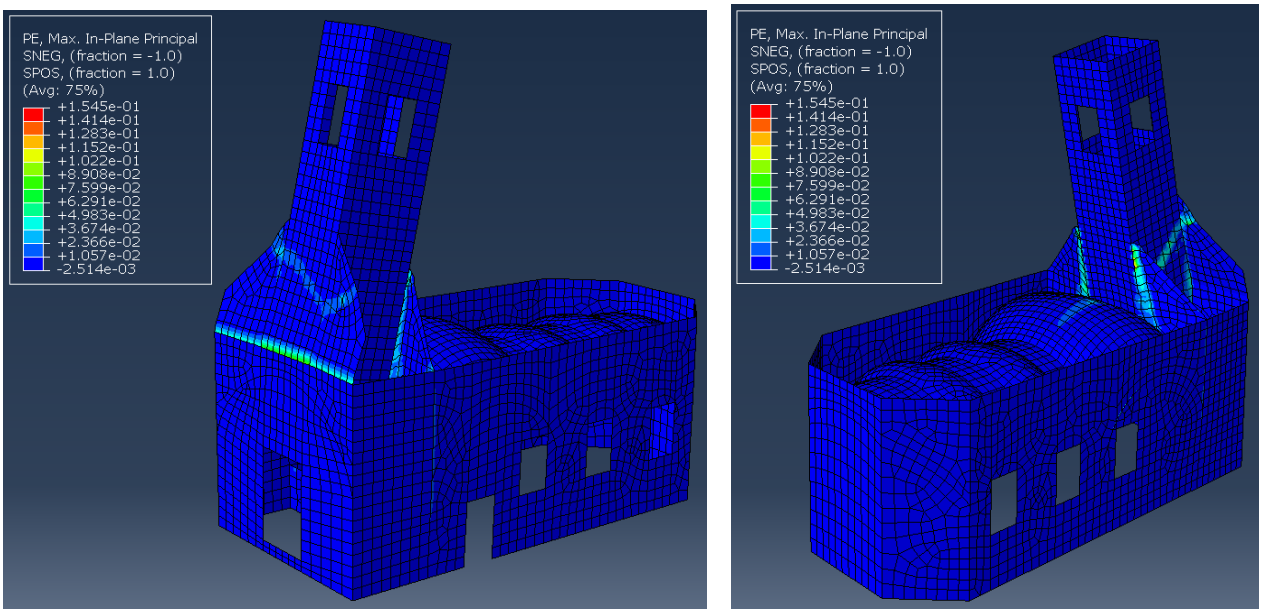

Figure 24: Distribution of maximal principal plastic strains for the pushover analysis in the +X direction

The mechanism that is observed is the rocking of the upper part of the bell tower. Only the part that is above the body of the church is rocking, which leads to the very clear horizontal crack in the front facade. Cracks also appear at the connection of the bell tower with the triangular masonry elements that support it on the sides. Cracks also form in the large vault that is the closest to the bell tower, probably due to the pushing of the bell tower against the vault.

The damage predicted by the numerical analysis corresponds partially to the observed damage on the church. The horizontal crack in the front facade predicted by the analysis is also visible in reality. The analysis also predicts cracks in the large vault near the bell tower, which is confirmed by the current state of the church, although it is hard to know which of these cracks were caused directly by the seismic action and which ones were caused by the fall of the bell tower on the vault. Similarities can even be seen in the shape of the cracks, as the curved cracks on the sides of the vault are also visible in reality (see figure 25).

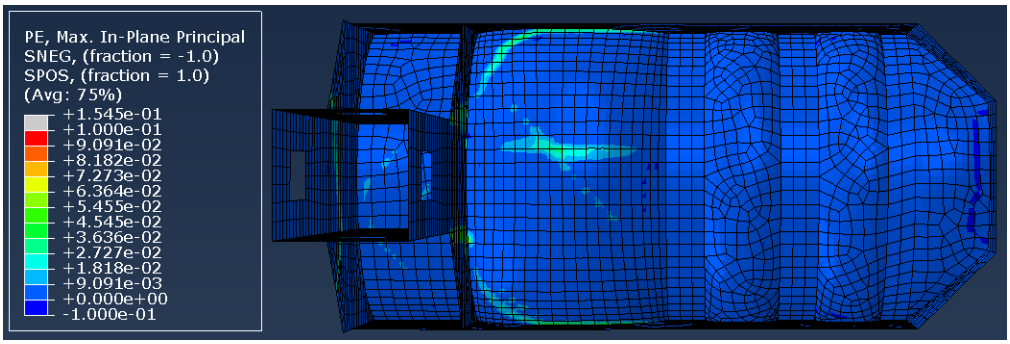

(a) Predicted cracks in the vaults from +X pushover analysis

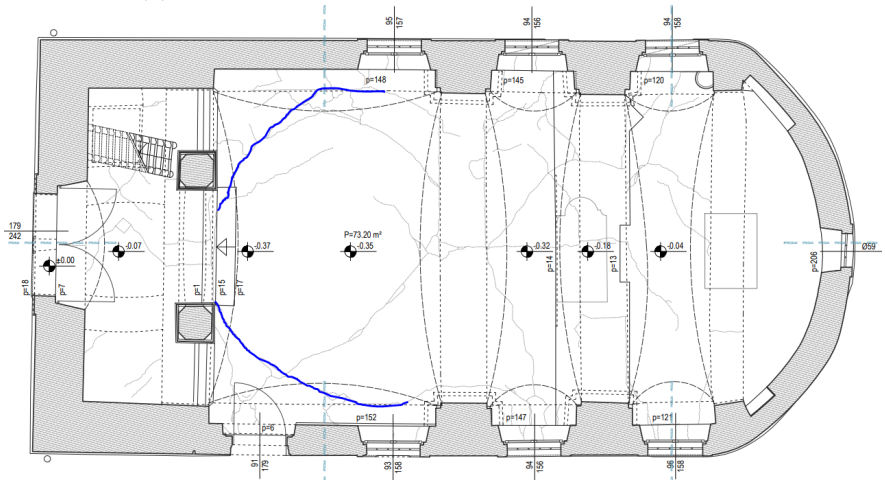

(b) Actual cracks in the vaults

Figure 25: Comparison of the cracks in the vault (similar crack shapes highlighted in blue)

The pushover curve (figure 26) is obtained by plotting the total base shear over the displacement of the top of the bell tower, which is the point that suffers the largest displacement of the whole model.

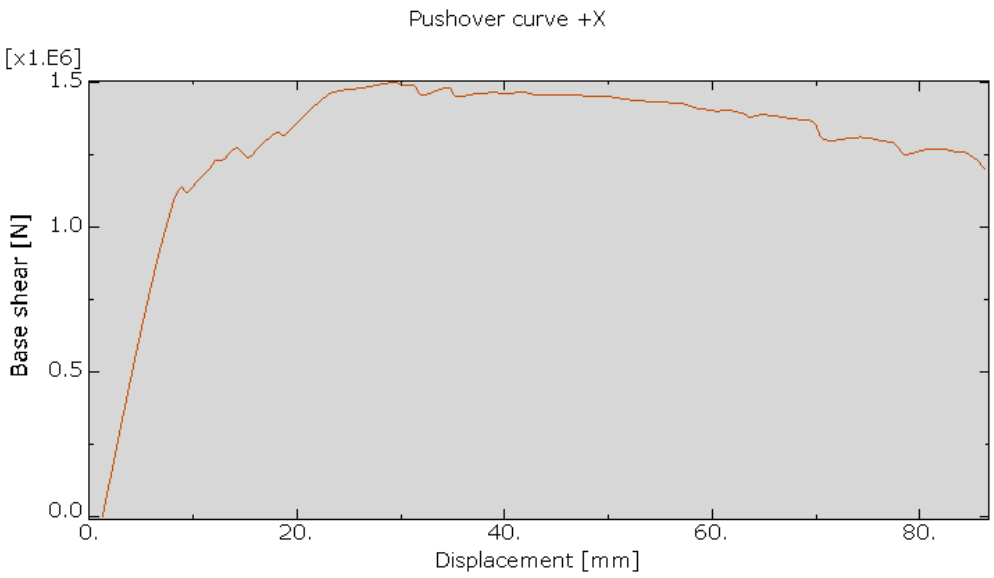

Figure 26: Pushover curve in the +X direction

The ultimate load that is reached is 1497 kN, at a top displacement of 29 mm. The ultimate displacement capacity, which is taken at 80 % of the ultimate load, is 86 mm. This displacement corresponds to a drift ratio of 0.64 %.

4.4.3 Pushover analysis in −X direction

After running the pushover analysis, it is possible to look at the deformed shape of the church (figure 27), and also the distribution of plastic strains (figure 28) to identify the failure mechanism.

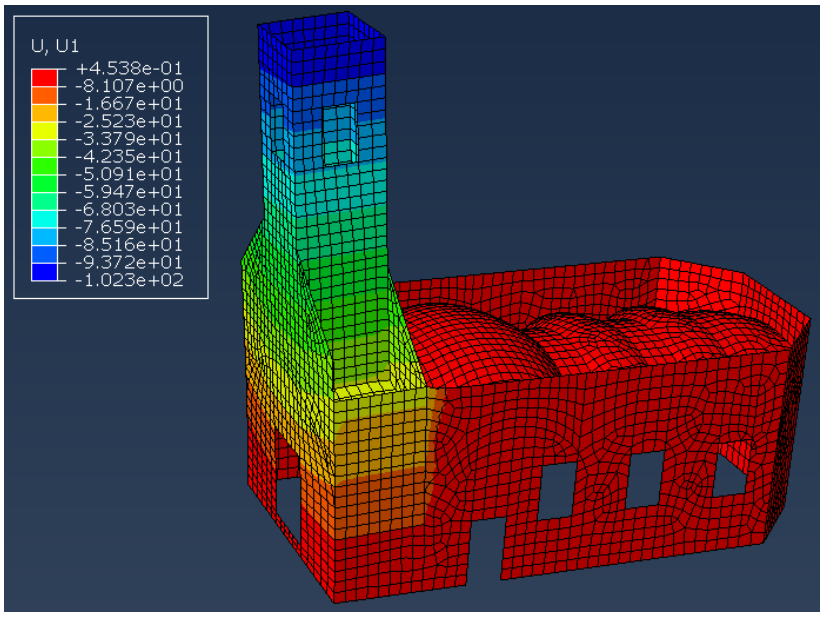

Figure 27: Displacement distribution for the pushover analysis in the −X direction

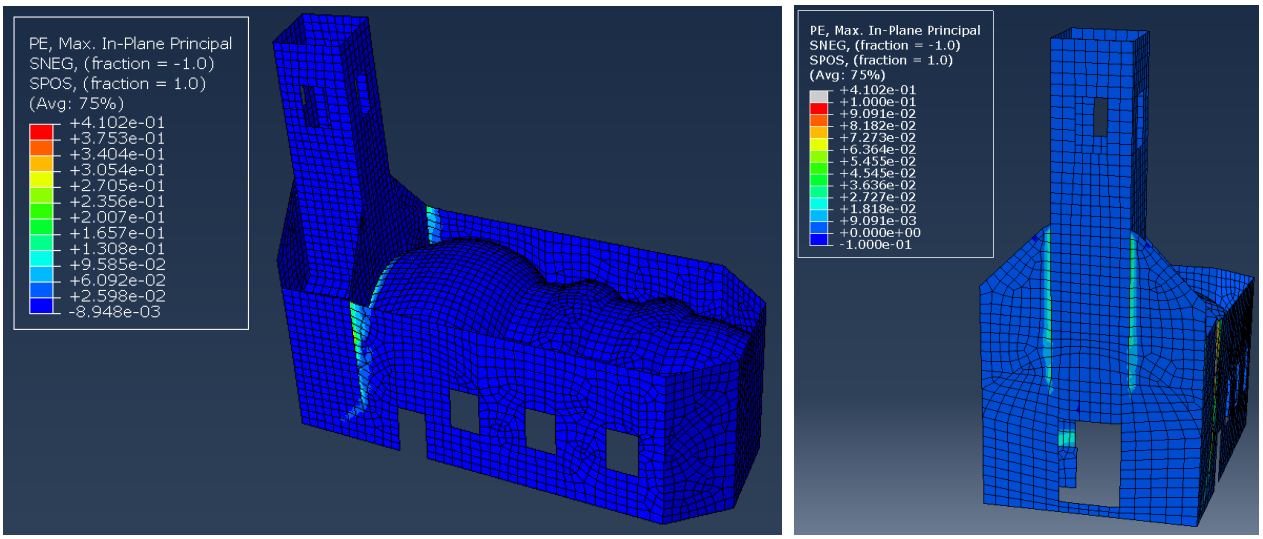

Figure 28: Distribution of maximal principal plastic strains for the pushover analysis in the −X direction

The mechanism that is observed is the rocking of the bell tower, but in the other direction. In this direction, the lower part of the bell tower is also moving, and we observe the separation of the bell tower and the rest of the church, with the formation of vertical cracks in the side walls (southeast and northwest facades). Cracks also appear at the connection between the vault and the bell tower, and in the front facade there are vertical cracks left and right of the bell tower.

The vertical cracks in the side walls are also visible on the church on both sides (figure 29). In the southeast wall, the crack seems to go through the side door. The predicted vertical cracks in the front facade also appeared in reality.

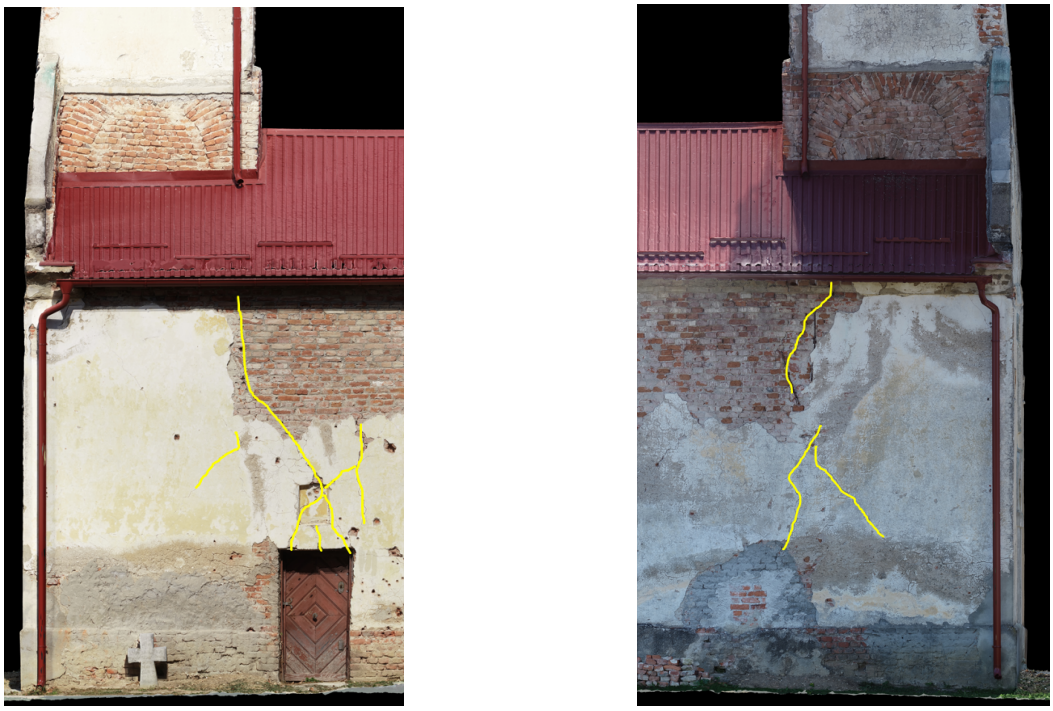

(a) Southeast wall **(b)** Northwest wall

Figure 29: Cracks at the connection between the bell tower and the rest of the church

The pushover curve (figure 30) is obtained by plotting the total base shear over the displacement of the top of the bell tower, which is the point that suffers the largest displacement of the whole model.

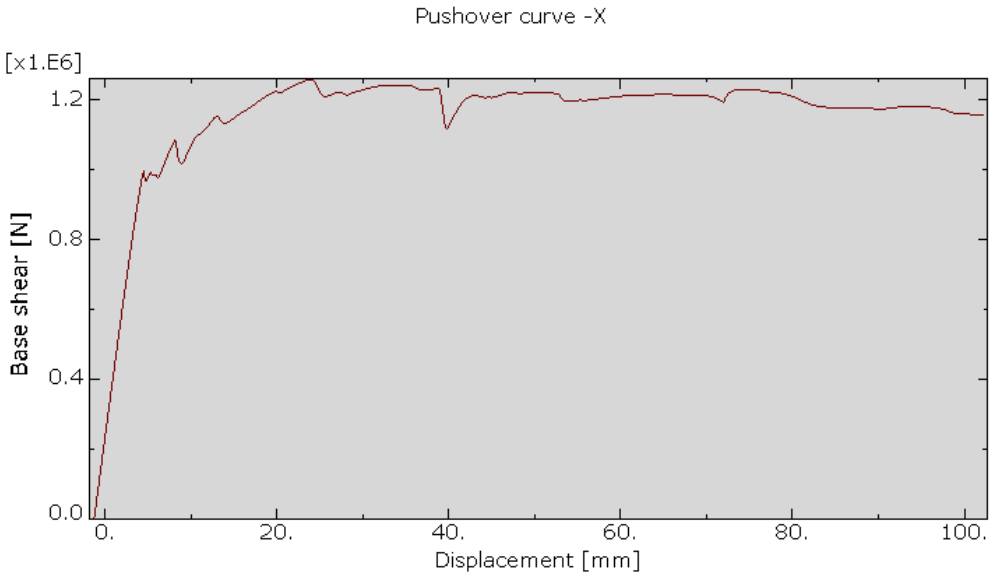

Figure 30: Pushover curve in the −X direction

The ultimate load that is reached is 1257 kN, at a top displacement of 24 mm. The analysis stops before the load capacity drops lower than 80 % of the ultimate load, so the last

calculated displacement is taken as the ultimate displacement capacity, which is 102 mm. This displacement corresponds to a drift ratio of 0.76 %.

4.4.4 Pushover analysis in +Y direction

After running the pushover analysis, it is possible to look at the deformed shape of the church (figure 31), and also the distribution of plastic strains (figure 32) to identify the failure mechanism.

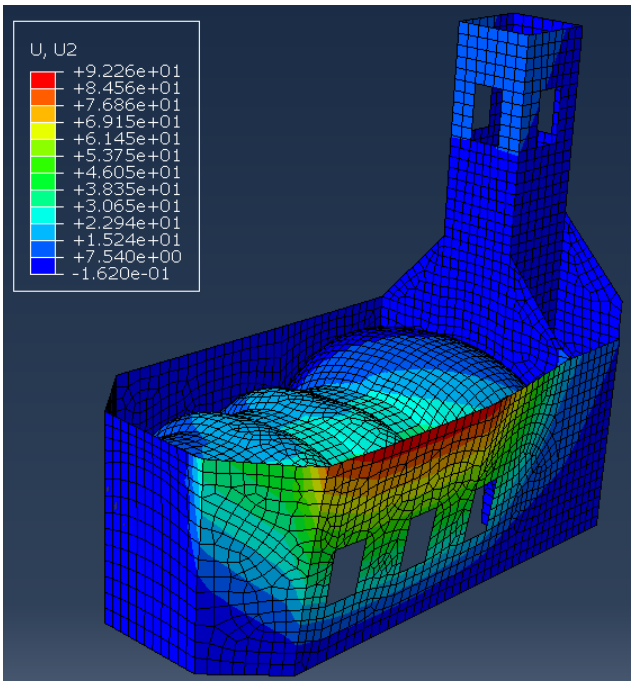

Figure 31: Displacement distribution for the pushover analysis in the +Y direction

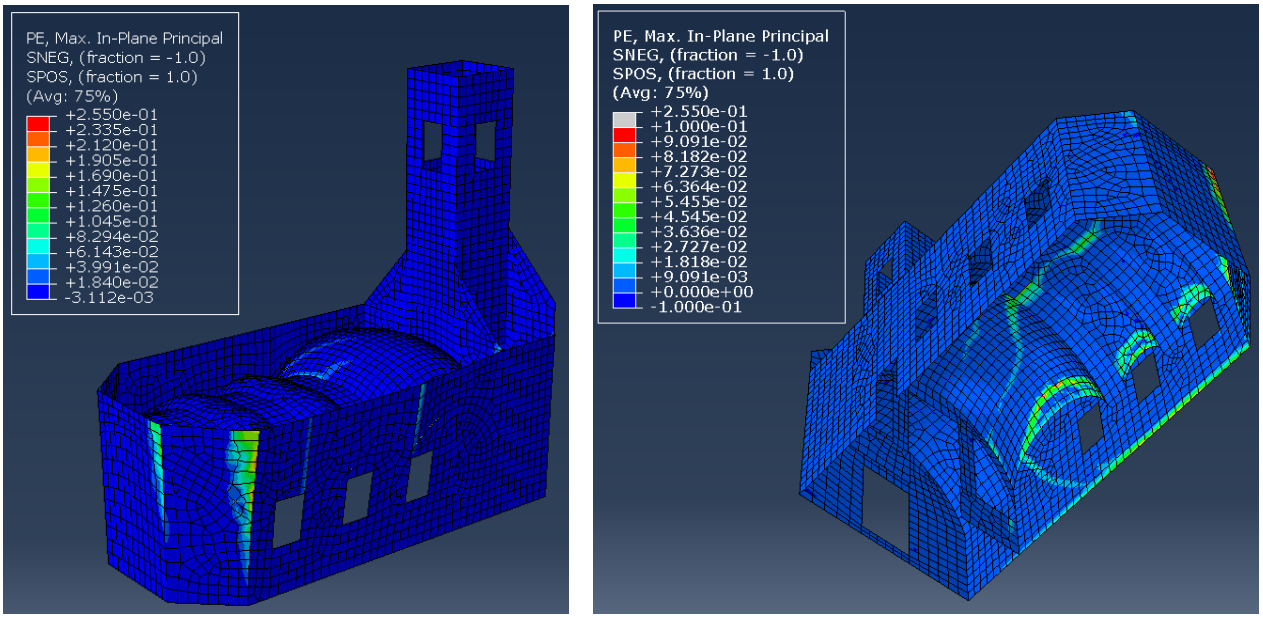

Figure 32: Distribution of maximal principal plastic strains for the pushover analysis in the +Y direction

The mechanism that is observed is the out-of-plane failure of the northwest wall. The rocking of the bell tower is not really happening in this direction, probably because of the triangular supports. The northwest wall suffers the combined action of the seismic force and the thrust of the vaults which pushes it outwards. Vertical cracks appear at the connection with the apse, as well as above the windows of this wall. Horizontal cracking is also observed at the base of the wall on the inside of the church, and many cracks appear in the vaults.

This predicted out-of-plane mechanism appears to be consistent with what happened in reality, because this northwest wall suffered some permanent deformation and is still slightly leaning outwards. The vertical cracks in the wall itself are also visible above some of the windows, on both the northwest and the southeast wall. Some cracks predicted in the vaults are also visible in reality (see figure 33).

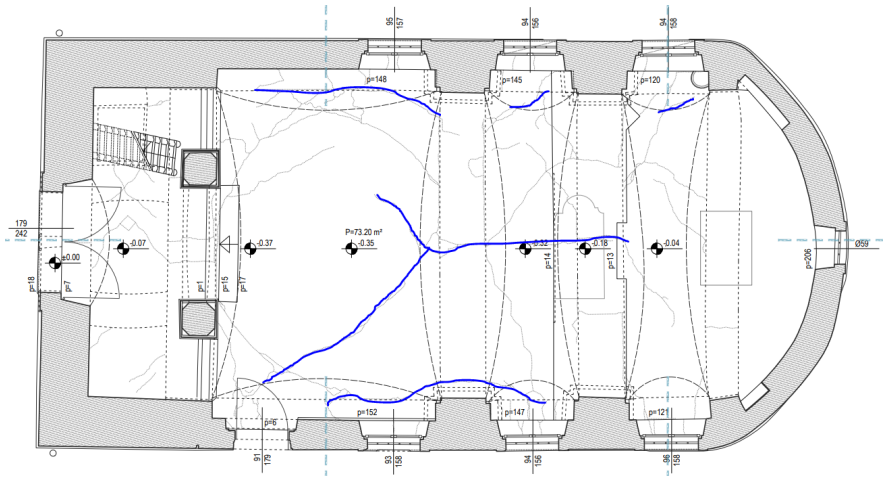

Figure 33: Cracks on the vaults that correspond to the predicted damage in the +Y direction

The pushover curve (figure 34) is obtained by plotting the total base shear over the displacement at the center of the top edge of the northwest wall, which is the point that suffers the largest displacement of the whole model.

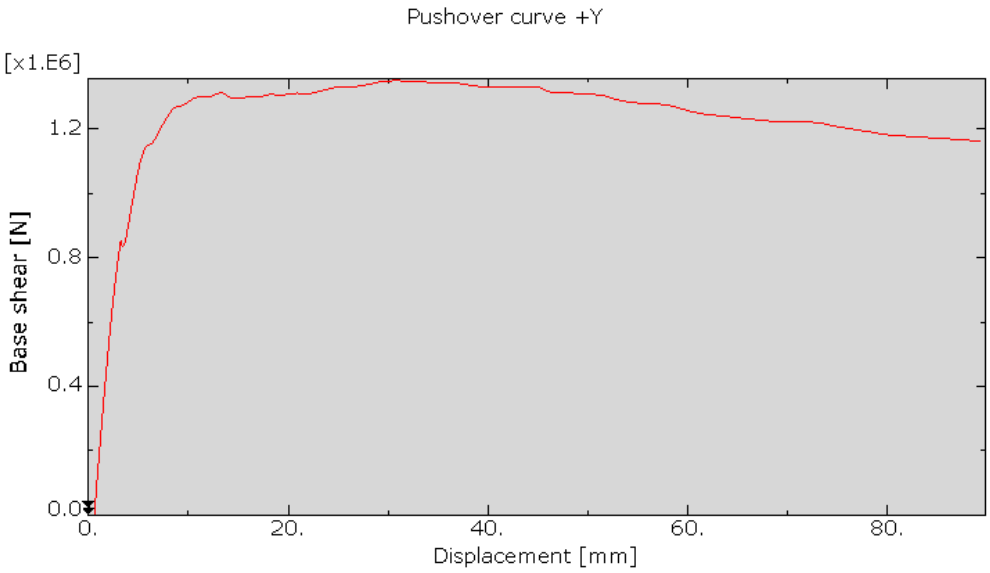

Figure 34: Pushover curve in the +Y direction

The ultimate load that is reached is 1351 kN, at a top displacement of 31 mm. The analysis stops before the load capacity drops lower than 80 % of the ultimate load, so the last calculated displacement is taken as the ultimate displacement capacity, which is 89 mm. This displacement corresponds to a drift ratio of 1.62 %.

4.4.5 N2 method

To compare the capacity of the church with the demand, the capacity curves for the SDOF system in all three directions are plotted on figure 35, along with the ADRS.

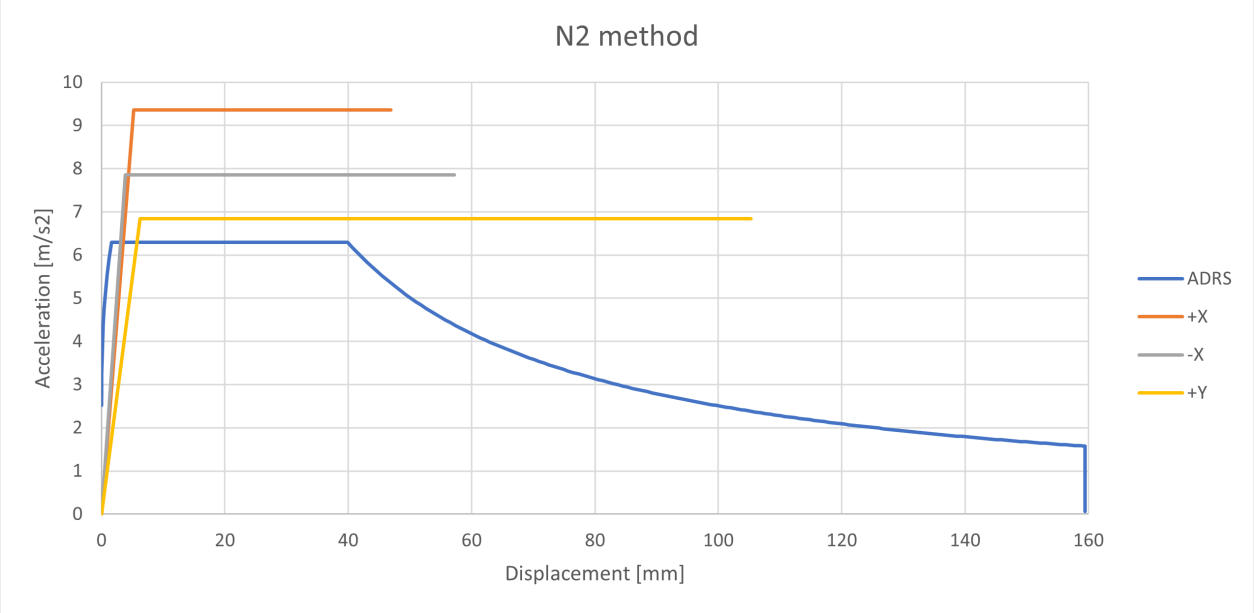

Figure 35: N2 method for the 3 studied directions

For all three directions, the force capacity is not exceeded, and the performance point of the structure is in the elastic region. The displacement demand δ_d^* and the acceleration demand a_d^*, which define the performance point, as well as the compliance factor for an acceleration-based verification CF_a and the period T^* are presented in table 7.

Direction	δ_d^* [mm]	a_d^* [m/s^2]	CF_a	T^* [s]
+X	3.5	6.3	1.49	0.15
−X	3.1	6.3	1.24	0.14
+Y	5.8	6.3	1.09	0.19

Table 7: Results of the N2 method in the three directions

The most critical direction, according to the acceleration-based compliance factor, is the +Y direction, although this one has the largest displacement capacity, so this mechanism is also far from the complete failure. The −X direction is more critical than the +X direction, which is expected since the thrust of the vault has a negative impact in this direction. The periods of the SDOF system are slightly larger than the periods of the respective modes (X : 0.08 s, Y : 0.17 s), which makes sense since the uncracked stiffness was used for the modal analysis, while in the pushover analysis the stiffness is reduced because of the cracking in the masonry structure.

It is quite surprising, and not really consistent with the observed damage on the church, that the load capacity of the church is not reached. Indeed, by looking at the many cracks and the failure of the bell tower, it would be expected that the load capacity is reached and that inelastic deformations happen. Multiple factors can explain this difference between the results of the numerical analysis and the observations on the church.

First of all on the demand side, for the peak ground acceleration, the design value for a return period of 475 years was taken, and not the peak value of the actual earthquake of 2020, so there could be a difference there. The assumption on the soil class is also quite uncertain.

On the capacity side, the simplifications used on the model could lead to differences with the real behaviour of the structure. The roof and spire mass, in particular, were estimated pretty roughly. But more importantly, there could be inaccuracies coming from the transformation from the MDOF system to the SDOF system. Indeed, the method is usually quite precise for regular buildings, where the mode shapes correspond well to the deformed shape of the pushover analysis. But in this case, the mode shapes that were used for the transformation into the SDOF system are quite different from the deformed shapes of the pushover analysis. This shows that the static analysis reaches its limits for such irregular buildings, and that a dynamic analysis would probably give better results. An improvement that could be done for the static analysis is the following : instead of using the modal parameters from the modal analysis, we could estimate the effective mass and participation factor based on the deformed shape from a pushover analysis on a linear elastic system. The deformed shapes would be closer to the ones of the inelastic pushover analysis and this would probably increase the effective mass, and therefore reduce the force capacity of the SDOF system.

Furthermore, the estimation of the material properties are also relatively uncertain. A parameter that has quite a big influence on the results and that can take a large range of values is the tensile strength of the masonry. This depends mainly on the quality of the mortar and in old buildings like this church, it is very much possible that the mortar quality is bad, which can often lead to high seismic vulnerability [4]. Therefore, it could be that the tensile strength of the masonry was overestimated.

To illustrate the influence of the tensile strength, the pushover analysis is carried out once again with half the tensile strength, i.e. 0.075 MPa. The N2 method is used and the results with the two different tensile strengths can be compared for the three directions of analysis.

The results for the three directions (figures 36, 37 and 38) show that the force capacity is indeed reduced a lot when the tensile strength is lower. The displacement capacity is also largely reduced, and the stiffness is slightly lower, because the cracks appear earlier. The force capacity is reached for all three cases, and the inelastic displacement demand can be calculated to then find the compliance factor for a displacement-based verification CF_d. The results are presented in table 8.

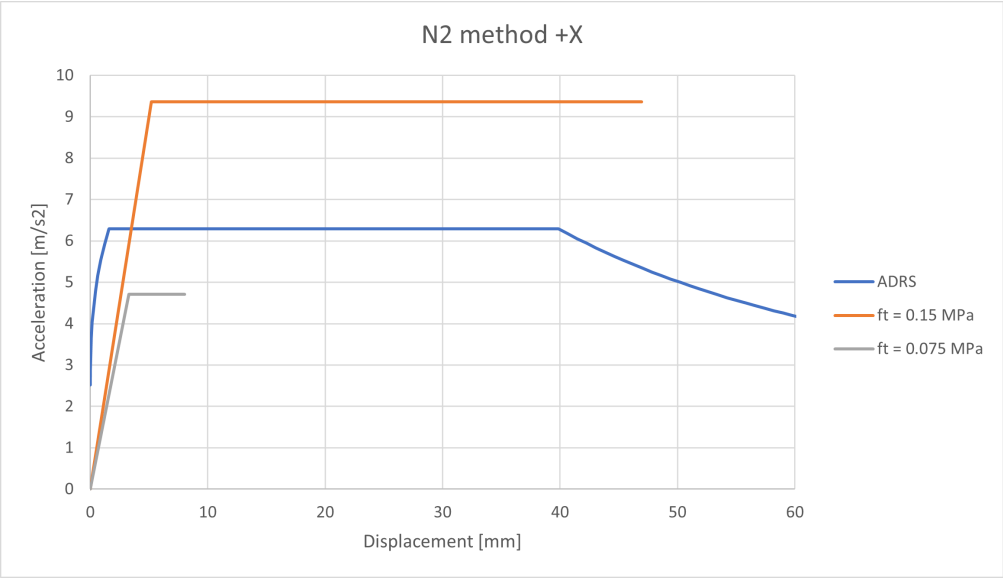

Figure 36: N2 method for the +X direction with different tensile strengths

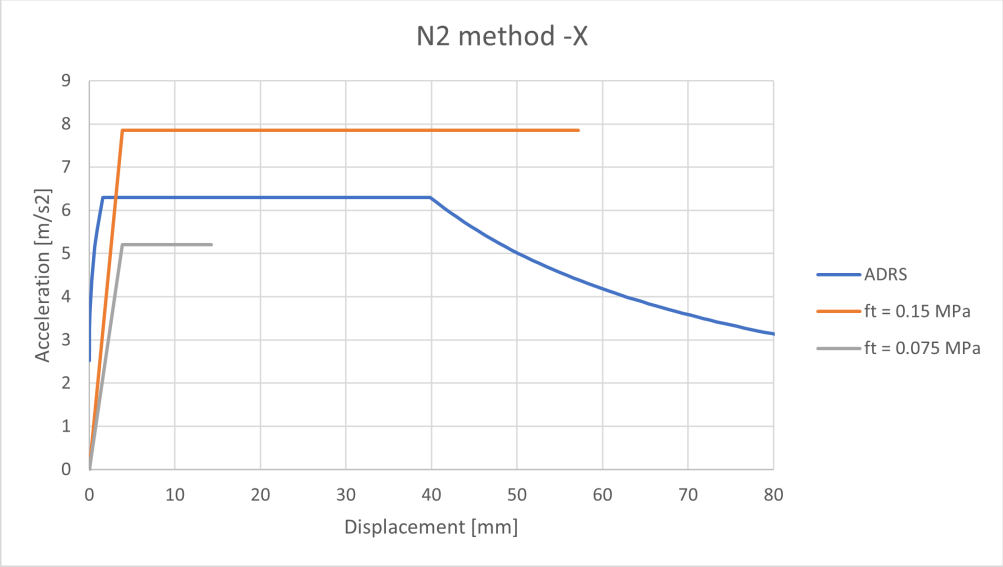

Figure 37: N2 method for the −X direction with different tensile strengths

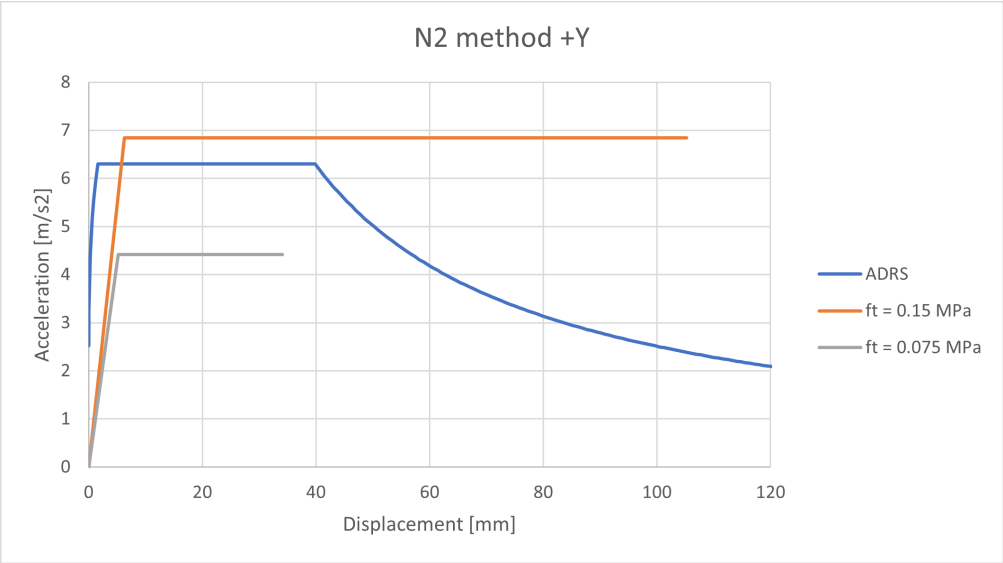

Figure 38: N2 method for the +Y direction with different tensile strengths

Direction	δ_d^* [mm]	a_d^* [m/s^2]	CF_d	T^* [s]
+X	6.6	4.7	1.21	0.17
−X	6.2	5.2	2.29	0.17
+Y	10.3	4.4	3.29	0.22

Table 8: Results of the N2 method in the three directions for the lower tensile strength

These results seem much more consistent with the observed damage on the church. Indeed, in all three directions, the church suffers inelastic deformations which explains the observed cracks in most of the masonry elements. But the displacement capacity is not reached, which means that the structural safety is still verified for the displacement-based assessment. The most critical direction of analysis for the displacement-based evaluation is the +X direction, while the other two directions have a relatively high margin before reaching the ultimate displacement capacity.

A lower tensile strength can even change the failure mechanism. The most obvious example is in the +Y direction, where we observe an in-plane failure of the southwest wall along with the out-of-plane mechanism of the northwest wall, while with the original tensile strength this was not the case (see figure 39).

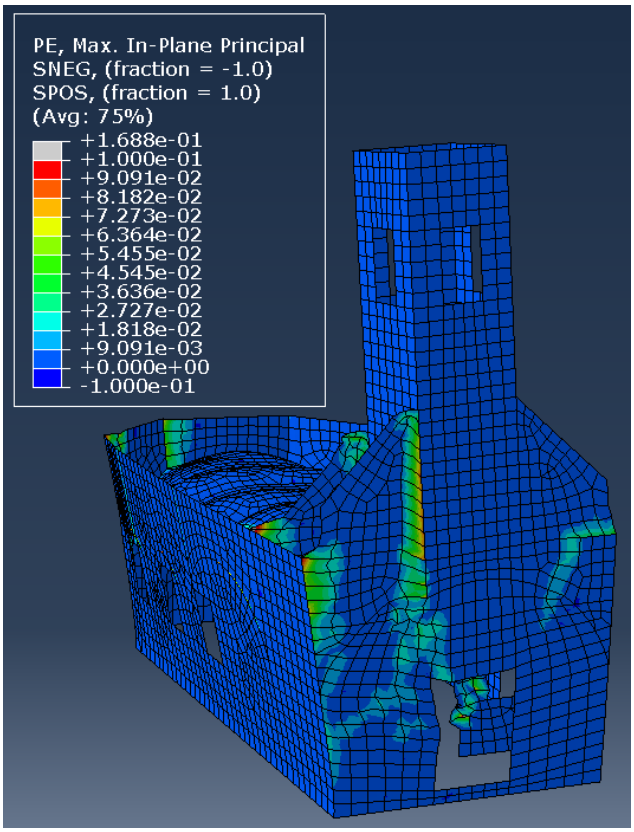

Figure 39: Failure mechanism in the +Y direction with the tensile strength of 0.075 MPa

This second analysis with the lower tensile strength confirms that this parameter has a big influence on both the force and displacement capacity. In order to get more reliable results, a more precise estimation of the material properties would be needed. Some tests should be carried out on the material of the church and the properties should be chosen to fit the results of the tests.

5 Hand calculations

By comparing the damage that is actually visible on the church and the predicted damage from the Finite element analysis, it is clear that some of the failure mechanisms are not predicted by the nonlinear analysis. Therefore, some of these mechanisms, which are mostly out-of-plane local mechanisms, are analysed with hand calculations.

5.1 Methodology

The method used for these hand calculations is described by Godio & Beyer [10]. The procedure is to write the moment equilibrium at the point of rotation of each mechanism. The destabilizing forces are the horizontal multiplier α multiplied by the weights W_i of the different blocks, and the stabilizing forces are the self weights of the blocks and, in some cases, a friction force. By stating that the horizontal displacement δ_i of the blocks is 0, we can find the horizontal multiplier at the onset of the mechanism α_0, and by stating that the horizontal multiplier α is 0 we can find the displacement corresponding to the loss of horizontal capacity δ_0. These two parameters allow us to draw the linear capacity curve for a MDOF system.

To compare the capacity to the demand, the MDOF system has to be transformed into an equivalent SDOF system. α_0 and δ_0 are transformed into the equivalent acceleration capacity a_0^* and equivalent displacement capacity δ_0^* with the following equations :

$$a_0^* = \alpha_0 \cdot g \cdot \frac{M_{tot}}{M^*} \tag{17}$$

$$\delta_0^* = \frac{\delta_0}{\Gamma} \tag{18}$$

With :

M_{tot} the total mass of all the blocks i moving in the mechanism :

$$M_{tot} = \sum_i M_i \tag{19}$$

M^* the effective mass of the SDOF system :

$$M^* = \frac{(\sum_i M_i d_i)^2}{\sum_i M_i d_i^2} \tag{20}$$

Γ the participation factor :

$$\Gamma = \frac{\sum_i M_i d_i}{\sum_i M_i d_i^2} \tag{21}$$

Where d_i is the normalized horizontal displacement at the centre of mass of each block i.

According to Eurocode 8, both the force-based verification and the displacement-based verification are possible. The force-based verification compares the acceleration capacity a_0^* to the acceleration demand a_d which, for a mechanism happening at ground level, is :

$$a_d = \frac{a_{gd} \cdot S}{q} \tag{22}$$

Where a_{gd} is the ground acceleration, S the parameter depending on the soil class and q the behaviour factor.

The compliance factor for the force-based verification can then be easily computed :

$$CF_a = \frac{a_0^*}{a_d} \tag{23}$$

For mechanisms happening higher than ground level, the acceleration demand can be calculated with the design response spectrum from SIA 261 [21], since the periods are known thanks to the modal analysis performed in Abaqus (section 4.4.1).

If the force capacity is exceeded, the displacement-based verification can be done. Some empirical relations allow to compute the displacement capacity δ_u^* and the yield displacement δ_y^* [10].

$$\delta_u^* = 0.4\delta_0^* \tag{24}$$

$$\delta_y^* = 0.4\delta_u^* \tag{25}$$

Then the period of the SDOF system T^* can be found, which allows to calculate the displacement demand δ_d with the elastic displacement response spectrum. The compliance factor for the displacement-based verification is then computed with equation (27).

$$T^* = 2\pi \cdot \sqrt{\frac{d_y^*}{a^*(d_y^*)}} \tag{26}$$

$$CF_d = \frac{\delta_u^*}{\delta_d} \tag{27}$$

For unreinforced masonry buildings, the behaviour factor is usually taken between 1.5 and 2 [1]. The list below contains a few general assumptions that were used in the calculations :

- The masonry does not have any tensile strength
- The masonry has infinite compressive strength
- Friction coefficient between masonry and mortar : $\mu = 0.6$
- Behaviour factor : $q = 1.5$

5.2 Southwest facade

A very clear crack pattern can be seen in the upper part of this facade (figure 40(a)) with horizontal, vertical and diagonal cracks. While some of these cracks are predicted by the pushover analysis in the +X direction (section 4.4.2), they could also indicate an out-of-plane mechanism as shown in figure 40(b), which did not appear in the numerical analysis. Therefore, it is also interesting to investigate this mechanism with hand calculations.

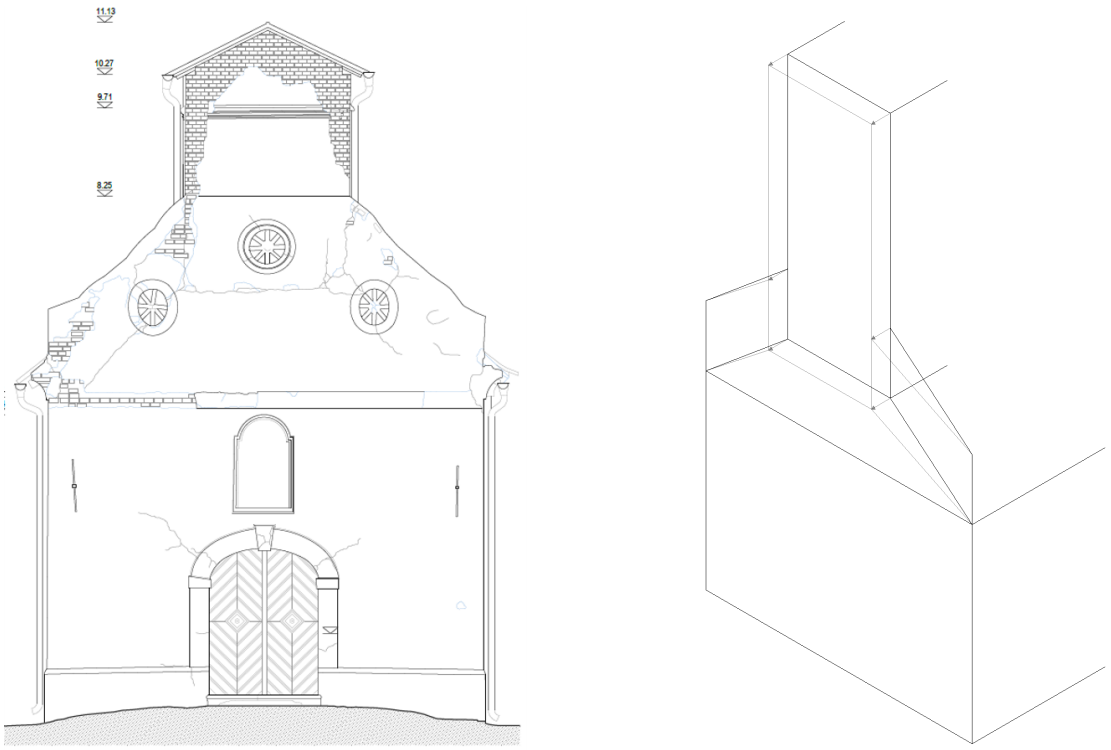

(a) Elevation of the facade

(b) 3D sketch of the mechanism

Figure 40: Southwest facade mechanism

The crack pattern suggests an out-of-plane mechanism with 4 rigid blocks. The trapeze at the bottom that rotates around its base, the top wall that stays vertical and only shifts horizontally, and the two parallelograms on the side that rotate around a vertical axis. We could also imagine that part of the side walls of the bell tower come along with the mechanism, depending on the interlocking of the bricks at the junction of the front wall and the side wall.

The sketch in figure 41 shows the kinematic model of rigid bodies with the weights and forces acting on it, as well as the displacements of the blocks.

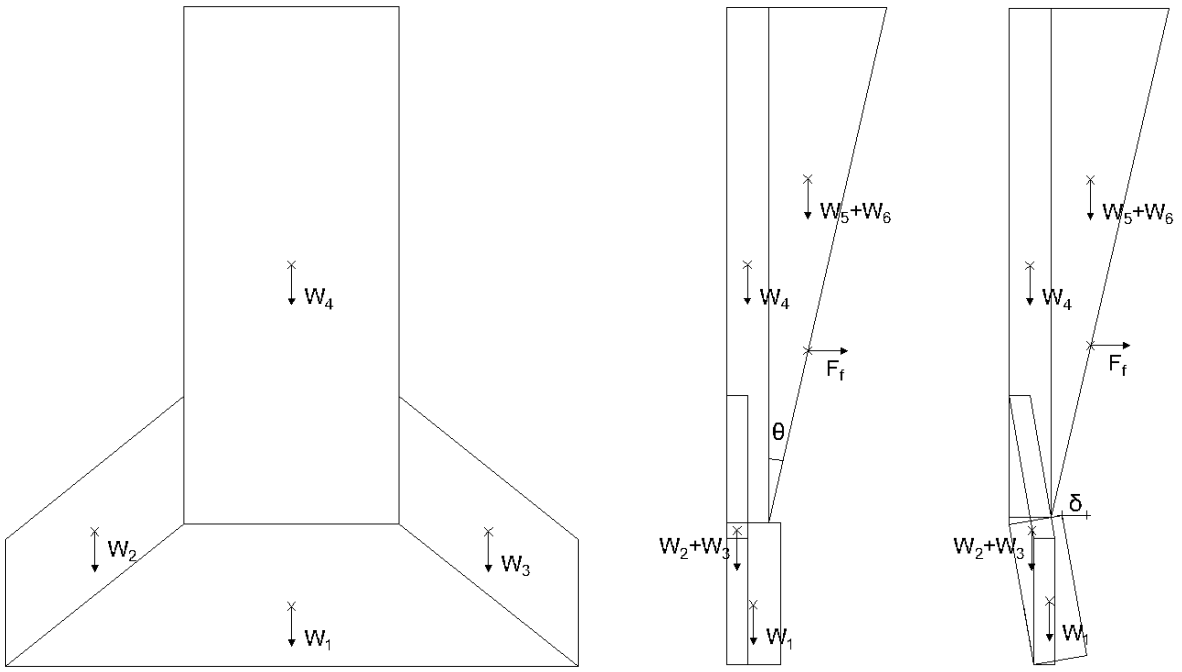

(a) Front view of the mechanism

(b) Side view of the mechanism

Figure 41: Mechanism of the southwest facade

It was assumed that a triangular part of the side walls of the tower could come along with the mechanism, with a variable angle θ (see figure 41(b)). By varying this angle, it is possible to find the most critical mechanism, i.e. the one with the lowest acceleration capacity.

The friction force F_f is assumed to be the weight of the side walls multiplied by the friction coefficient, and acts at the third of the height of the side walls, since the friction distribution over the height has a triangular profile with the maximum friction at the bottom and no friction at the top. However, this simple friction model would mean that when the angle θ tends to 0, the friction force tends to 0 since the side wall has no weight anymore. But in reality this cannot be true because there would still be friction restraining the movement of the front wall because of the interlocking of the bricks at the junction of the front wall and the side walls. But this interlocking of the bricks is complex to identify based on the available plans and photos, so a simpler assumption was made : the friction force should have a minimal value corresponding to half of the weight of the common part of the front wall and the side walls, multiplied by the friction coefficient.

The moment equilibrium at the base of the trapezoidal block (lower left corner in figure 41(b)) can then be written :

$$\sum M = \alpha \cdot \sum_i W_i \cdot z_i - \sum_i W_i \cdot (x_i - \delta_i) - F_f \cdot z_{F_f} = 0 \tag{28}$$

5.2.1 Results

The most critical mechanism for the acceleration capacity happens when $\theta = 4.7°$. Then we get the following results :

$$\alpha_0 = 0.157$$

$$\delta_0 = 0.71\,m$$

After transforming it into a SDOF system, we get the following acceleration capacity and displacement capacity :

$$a_0^* = 1.74\,m/s^2$$

$$\delta_0^* = 0.60\,m$$

Since this mechanism happens at approximately 5.5 m above the ground, the design response spectrum can be used to determine the acceleration demand. According to the modal analysis that was performed on the church model (section 4.4.1), the fundamental mode in the X direction has a period of 0.23 s, which is in between the corner periods T_B and T_C. Then the compliance factor for the force-based assessment can be calculated.

$$a_d = 2.5 \cdot \frac{a_{gd} \cdot S}{q} = 4.2\,m/s^2$$

$$CF_a = 0.41$$

Since the force-based verification is not verified, the displacement-based verification should be carried out.

$$CF_d = 1.87$$

So this shows that it is very likely that this mechanism has started to develop during the earthquake, which explains the observed cracks. However, the displacement capacity is not reached, which is also consistent with the damage, since this mechanism did not lead to the complete failure.

An interesting comment was brought by Martina Vujasinovic, who said that some photos from before the earthquake of December 2020 showed that these cracks were already there (some of them are vaguely visible in figure 1). But according to what she said, it is unlikely that they appeared during an earlier earthquake, since the region of Petrinja had not suffered similar events for decades. This means that these cracks must have been caused by another horizontal action which is unknown for now. But it does not exclude the possibility that this mechanism happened again during the earthquake of 2020.

5.3 Bell tower

The most obvious failure mechanism that is not captured by the numerical analysis is the failure of the bell tower at the level of the windows. In the pushover analysis in every direction, the failure always occurs at a lower level, so it is interesting to imagine what mechanism lead to this failure of the bell tower. By comparing the photos before (figure 1) and after the earthquake (figure 5), we can see that the tower failed at the base of the windows. This

suggests that the piers next to the windows started rocking simultaneously, while the block above the windows moved sideways without rotating (see figure 42).

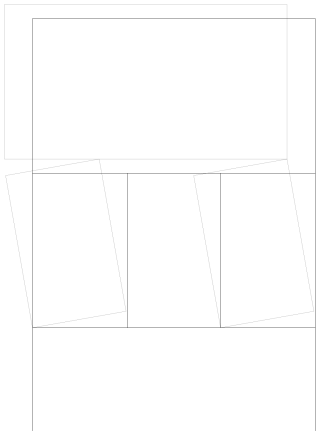

Figure 42: Sketch of the bell tower mechanism

This mechanism could happen in both X and Y direction, but since the piers are slightly more slender in the Y axis, it is more critical and only this direction will be analysed. The mass of the spire is assumed to be 2 tons, and the center of mass is assumed to be 2 m above the top of the masonry tower. The kinematic model of rigid bodies with the weights is shown in figure 43.

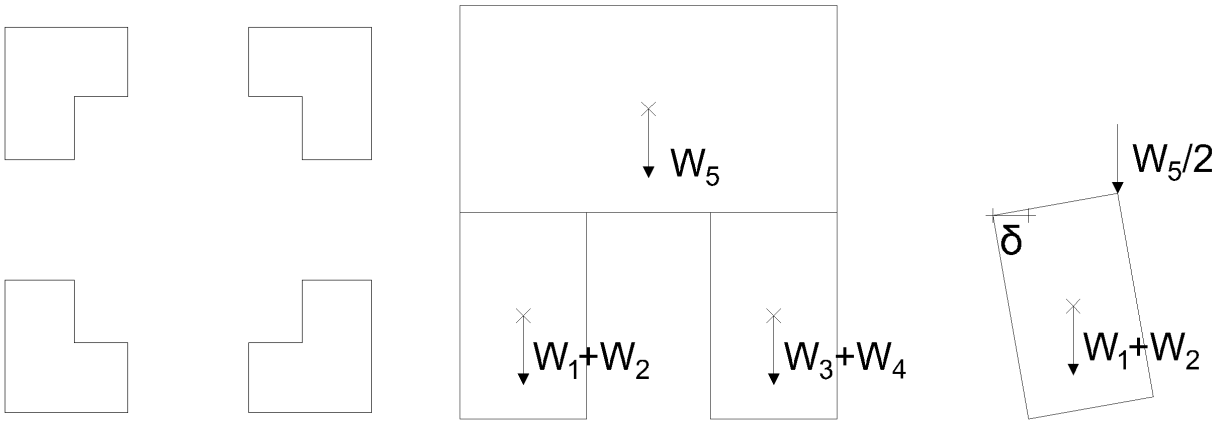

(a) Cross section of the piers

(b) Side view of the mechanism

Figure 43: Bell tower mechanism

Since it is symmetric, only half of the mechanism is analysed for a simpler moment equilibrium. It is assumed that half of the weight of the upper block and of the spire is acting on each side of the tower. When the piers start rocking, the weight of the upper block and of the spire is transferred to the piers at the point of contact, which is the upper right corner of the pier in figure 43(b) (because of the infinite compression strength assumption).

The moment equilibrium at the lower left corner of the pier can then be written :

$$\sum M = \alpha \cdot \sum_i W_i \cdot z_i - \sum_i W_i \cdot (x_i - \delta_i) = 0 \tag{29}$$

5.3.1 Results

$$\alpha_0 = 0.374$$

$$\delta_0 = 0.89\,m$$

After transforming it into a SDOF system, we get the following acceleration capacity and displacement capacity :

$$a_0^* = 3.97\,m/s^2$$

$$\delta_0^* = 0.80\,m$$

Since this mechanism happens at approximately 10.5 m above the ground, the design response spectrum can be used to determine the acceleration demand. According to the modal analysis that was performed on the church model (section 4.4.1), the fundamental mode in the Y direction has a period of 0.17 s, which is in between the corner periods T_B and T_C. Then the compliance factor for the force-based assessment can be calculated.

$$a_d = 2.5 \cdot \frac{a_{gd} \cdot S}{q} = 4.2\,m/s^2$$

$$CF_a = 0.95$$

Since the force-based verification is not verified, the displacement-based verification should be carried out.

$$CF_d = 3.26$$

This result is not exactly consistent with the observed damage, since the calculation predicts that the displacement capacity is not exceeded, while in reality the bell tower failed entirely. There can be many reasons to explain this difference between the results of the analysis and the actual damage.

First of all, the infinite compressive strength assumption can lead to a slight overestimation of the force capacity and displacement capacity. In addition, the dimensions of the different elements and the mass of the spire are estimated very roughly, since this upper part of the bell tower does not appear in the blueprints of the church. It is also possible that the assumed mechanism is not exactly the one that led to the failure. Pure rocking was assumed, but actually it could be that the blocks start sliding after they begin to rock, with the failure mechanism being more shear dependant.

5.4 Local mechanism in the apse

On the inside of the apse, we can see two very clear diagonal cracks that form an X shape. Usually this type of cracks suggests an in-plane shear mechanism. But in this case, the cracks are only visible on the inside and not on the outside of the wall (figure 44). This could indicate that it might be an out-of-plane mechanism with four triangular blocks joining each other in the center, where the window is, with this center point moving inwards (see figure 45).

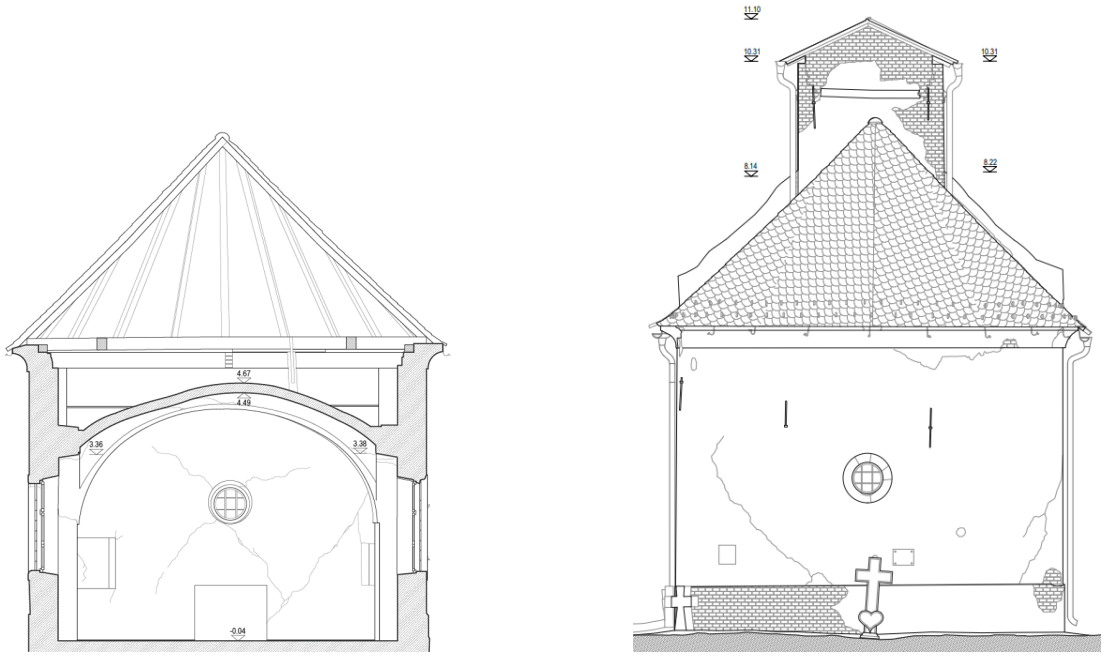

(a) Transverse section showing the inside of the apse wall

(b) Elevation of the outside of the apse wall

Figure 44: Crack patterns in the apse

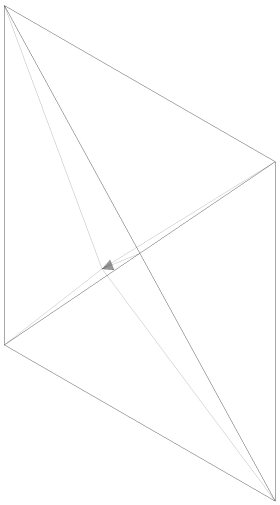

Figure 45: 3D sketch of the local apse mechanism

This is just a hypothesis, of course it is also possible that these cracks are due to an in-plane shear mechanism and that for some unknown reason the cracks did not appear on the outside.

The principle of virtual work was used for this mechanism, since not all the blocks rotate around the same axis. The curvature of the apse is neglected in these calculations. The kinematic model of rigid bodies with the weights is shown in figure 46.

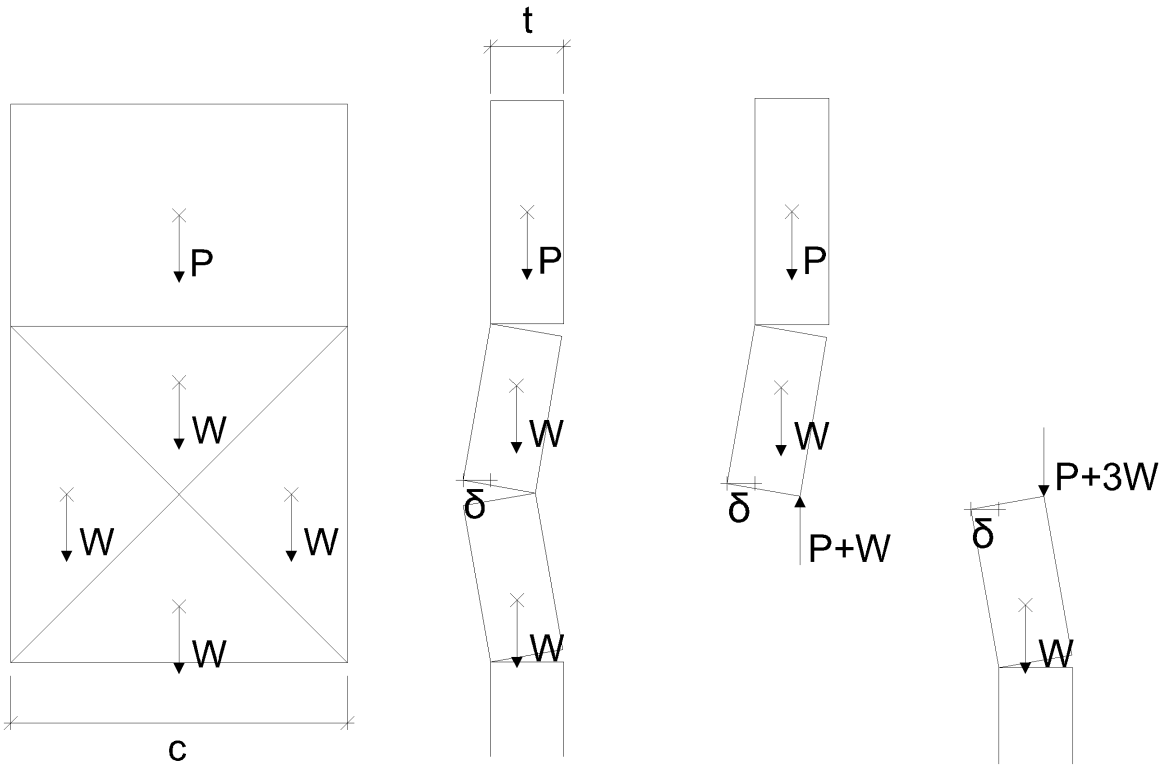

(a) Front view of the mechanism

(b) Vertical section in the middle of the mechanism

(c) Separation of the upper and lower triangle

Figure 46: Loacal apse mechanism

It is assumed that the 4 triangles are identical, with a variable base c (see figure 46(a)). There is also the weight of the remaining top part of the wall P that is acting on top of the triangles, which also depends on c. We can then compute the external work, which is for each triangle the horizontal multiplier multiplied by its weight and the displacement of its centre of mass.

$$W_e = 4 \cdot \alpha \cdot W \cdot \frac{\delta}{3} \tag{30}$$

Then we can compute the internal work, which is for each triangle the stabilizing moment multiplied by the rotation of the triangle. For the left and right triangles, since the rotation is around the vertical axis, the weights of the blocks are not directly stabilizing forces since they are vertical, so it is assumed that these two triangles do not have stabilizing forces. This is of course not exactly true because the part of the wall left and right of the mechanism would still restrict the triangles from rotating. For the top triangle, the stabilizing moment is the

reaction due to the weight of the top wall P and the self-weight of the triangle W multiplied by its lever arm, which is the thickness of the wall because of the infinite compression strength assumption. For the bottom triangle, the stabilizing moments are the weight of the top wall P and the self-weight of the other 3 triangles multiplied by their lever arm (again, the thickness of the wall).

$$W_i = -(W + P) \cdot (t - \delta) \cdot \frac{\delta}{c/2} - (3 \cdot W + P) \cdot (t - \delta) \cdot \frac{\delta}{c/2} \tag{31}$$

We can then write the principle of virtual work.

$$W_e + W_i = 0 \tag{32}$$

$$4 \cdot \alpha \cdot \ W \cdot \frac{\delta}{3} - (W + P) \cdot (t - \delta) \cdot \frac{\delta}{c/2} - (3 \cdot W + P) \cdot (t - \delta) \cdot \frac{\delta}{c/2} = 0 \tag{33}$$

By dividing by δ and multiplying by $c/2$, we get the following equation :

$$\frac{2}{3} \cdot \alpha \cdot \ W \cdot c - (4 \cdot W + 2 \cdot P) \cdot (t - \delta) = 0 \tag{34}$$

5.4.1 Results

By varying the length c, we realise that the larger c becomes, the smaller the acceleration capacity becomes. The upper bound for c, given by the size of the wall, is approximately 4 m. Then we get the following results :

$$\alpha_0 = 1.17$$

$$\delta_0 = 0.54\, m$$

After transforming it into a SDOF system, we get the following acceleration capacity and displacement capacity :

$$a_0^* = 11.5\, m/s^2$$

$$\delta_0^* = 0.18\, m$$

This mechanism occurs at ground level, so the acceleration demand is computed with equation (22). The compliance factor for the force-based verification is then :

$$CF = 6.86$$

In this case, the compliance factor is significantly larger than 1. Some assumptions (e.g. the fact that there is no stabilizing moment for the side triangles) are on the safe side. All of this leads to the conclusion that this mechanism is not likely to happen during an earthquake, even if the model that was used is not entirely exact. It is more likely that the visible cracks were caused by an in-plane shear mechanism.

5.5 Overturning of the apse

The visible cracks below and above the window that is closest to the apse in the southeast facade could suggest an out-of-plane overturning of the whole apse (figure 47).

(a) Cracks below and above the window closest to the apse

(b) Sketch of the mechanism

Figure 47: Apse overturning mechanism

Based on these cracks, it is assumed that part of the side walls come along with the mechanism. Diagonal cracks are assumed under and over the windows. The apse vault and the first arch also come along with the overturning mechanism. The horizontal thrust F_h of the second vault acts as a destabilizing force. The thrust is estimated with simple statics by considering only the self weight of the vault.

The moment equilibrium at the base of the apse can then be written :

$$\sum M = \alpha \cdot \sum_i W_i \cdot z_i + F_h \cdot z_{Fh} - \sum_i W_i \cdot (x_i - \delta_i) = 0 \tag{35}$$

5.5.1 Results

$$\alpha_0 = 0.299$$

$$\delta_0 = 1.65\,m$$

After transforming it into a SDOF system, we get the following acceleration capacity and displacement capacity :

$$a_0^* = 3.06\,m/s^2$$

$$\delta_0^* = 0.92\,m$$

This mechanism occurs at ground level, so the acceleration demand is computed with equation (22). The compliance factor for the force-based verification is then :

$$CF = 1.83$$

The force-based assessment leads to the conclusion that the structural safety is verified. This could mean that the observed cracks are caused by another mechanism, like the out-of-plane mechanism of the northwest and southeast walls, as it was shown by the pushover analysis in the Y direction (section 4.4.4).

6 Retrofitting propositions

The combination of the observed damage, the numerical analysis and the hand calculations allows to identify the most vulnerable and critical parts of the church structure that would need to be retrofitted in order to guarantee the structural safety in the case of future seismic events.

The results of the pushover analyses with the original tensile strength of 0.15 MPa would not justify any strengthening measure, since the structure has a sufficient load capacity and remains elastic in all three directions. However, the influence of the tensile strength has been shown in section 4.4.5 and the force capacity is reached in all directions with a tensile strength of 0.075 MPa, even though the displacement capacity is still sufficient. If the tensile strength was even lower, which is not totally unlikely, the displacement capacity could very well not be enough anymore. The results of the hand calculations do not entirely justify the retrofitting of the structure either, since none of the mechanisms lead to a complete failure. Either the force-based, or at least the displacement-based assessment is verified for every studied mechanism.

But the damage observed on the church still indicates that some retrofitting interventions are probably needed. Especially when similar damage is predicted in the analyses and observed in reality, it is a strong indication that some action is necessary. Retrofitting solutions are proposed for three different damaged elements : the connection between the bell tower and the rest of the church, the bell tower and the vaults. This is not an exhaustive list of all the retrofitting actions that should be taken. With more refined and precise analysis methods, some of them could prove to be unnecessary, and some other necessary interventions could come to light. But based on this analysis, the three elements mentioned above will be investigated.

The aim is to propose some solutions and discuss their effectiveness as well as their adequacy in the case of a historical church. Before implementing any of these interventions, the behaviour of the retrofitted structure should be analysed to check if the intervention serves its purpose and does not create additional problems. But the analysis of the retrofitted structure is not carried out in this study and could be done in further works.

Since this church is a building of architectural heritage, its historical and cultural value should be maintained as much as possible. Therefore, the structural effectiveness of the intervention is not the only important criterion in the choice of the retrofitting solution. According to the ICOMOS-ISCARSAH Guidelines [17], the following criteria should be taken into account when designing a retrofitting intervention :

- **Compatibility** of the intervention with the original materials and techniques
- **Durability** of the repair or reinforcing materials
- **Non-invasiveness** of the intervention

- **Removability** of the measures in the eventuality that a more advanced or more respectful intervention is discovered in the future

The principle is to choose an intervention that ensures the structural safety and satisfies most of these criteria. Satisfying all of them simultaneously is often difficult or even impossible, but the goal is always to favor the minimal intervention.

Before addressing the proper retrofitting, whose aim is to increase the resistance of the structure compared to before the earthquake, the rehabilitation of the masonry structure should be dealt with. The difference between the rehabilitation and the retrofitting is that the rehabilitation aims to repair the existing damage so that the structure recovers its initial strength and stiffness, but without increasing its performance significantly compared to its original configuration.

The rehabilitation consists mainly of repairing the cracks that appeared in all the masonry elements. Indeed, cracks reduce the stiffness of the masonry structure and can therefore lead to higher displacements in case of future earthquakes which could potentially exceed the displacement capacity. For this reason as well as for aesthetic reasons and to provide a sense of safety to the user, the cracks should be repaired. If a crack only runs through the mortar joints, the repointing of the mortar should be sufficient [14]. This method consists of removing the outer layer of damaged mortar to replace it with a new one. This seals the cracks and should allow the masonry members to recover their stiffness and strength. This method can be carried out on both sides of a wall, but one side after the other, not simultaneously. The plaster covering the masonry should be removed before performing this operation, and the execution should be done very carefully and as much as possible with traditional tools so as to avoid damaging the existing materials more. If a crack runs through the entire thickness of an element, the mortar repointing could be combined with grout injections [14], in order to seal the crack in depth and not just on the surface.

In the case of cracks that run not only through the mortar but also through the bricks, the local dismantling and reconstruction of the wall is preferred [14]. The damaged bricks should be replaced with new ones and the masonry should be reconstructed as closely as possible to the original configuration in order to recover the stiffness and strength. Because of the plaster layer, it is difficult to tell which cracks are localized in the mortar joints and which led to a rupture of the bricks. But some cracks in the vaults are really widely open, and therefore it is very likely that they need to be locally dismantled and rebuilt, unlike most cracks in the walls that look thinner and are probably localized in the mortar. Finally it should be noted that for both techniques mentioned, the compatibility of the new and original materials is a crucial aspect for the effectiveness of this rehabilitation method.

6.1 Bell tower - wall connection

The pushover analysis in the $-$X direction (section 4.4.3) predicts the separation of the bell tower and the rest of the church, with the formation of vertical cracks in the southeast and northwest walls. This prediction of the numerical analysis is corroborated by the presence of

similar cracks in the church.

The goal of the intervention is therefore to connect these two parts of the church together, so that the whole church behaves as a monolithic ensemble. This can be achieved by the addition of longitudinal steel ties inside the southeast and northwest walls, above the windows (see figure 48). The procedure consists of inserting ties into holes drilled in the walls parallel to the wall surface, and anchoring them at both ends with simple devices like bars or plates [14]. These ties would connect both parts together thanks to their tensile strength and could transfer part of the horizontal forces (caused by the mass of the bell tower) to the rest of the church and therefore increase its total strength. It could also avoid some potential pounding between the bell tower and the rest of the church.

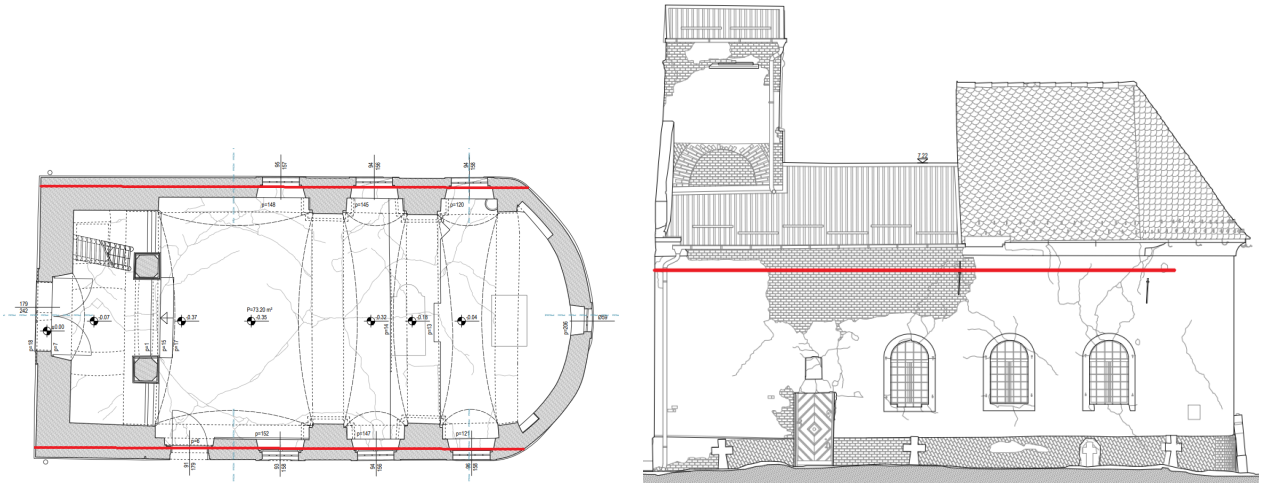

(a) Plan view **(b)** Elevation

Figure 48: Introduction of the steel ties

A potential problem that this measure could create is the fact that it would probably increase the horizontal forces in the rest of the church which could become more vulnerable. It could also lead to a different failure mechanism where only the top part of the bell tower would rock, similarly to the result of the pushover analysis in the +X direction.

This retrofitting method presents many advantages. Firstly, it shows good compatibility with the masonry, since it does not change the mass nor the stiffness significantly. Secondly, it is easily removable since the ties are not bonded to the masonry. Finally it is non-invasive given that it is not visible except for the anchors, and it is a traditional retrofitting method that has been used for many decades [14]. The downside lies in the durability, because the ties are prone to corrosion. But the state of the ties can be easily controlled periodically.

A lot of attention has to be put into the anchoring details when implementing this method. While the anchoring on the southwest side should not be too difficult, the curvature of the apse could complicate the anchoring on the northeast side, because there is no perpendicular surface to place the anchoring device. This should be investigated more in detail if this retrofitting method were to be chosen.

6.2 Bell tower

During the earthquake of 2020, the bell tower failed at the level of the windows, and the upper part of the tower and the spire fell down. This failure was not predicted by the finite element analysis, while the hand calculations showed that the mechanism should have started happening, but not led to a complete failure. This discrepancy between the results of the analyses and what happened in reality could indicate that there is a lack of connection of the masonry elements around the windows. The upper part of the bell tower will have to be rebuilt, and the opportunity should be taken to strengthen the bell tower so that this failure can be avoided in case of a future earthquake.

Given the failure mechanism that probably led to the failure (described in section 5.3), the aim of the retrofitting strategy should be to avoid the rocking of the piers surrounding the windows. This could probably be achieved by introducing vertical prestressing bars inside the walls of the tower, in the 4 corners (see figure 49). This would induce vertical compressive stresses in the masonry and would therefore avoid the uplift of the piers. The compression would at the same time improve the shear resistance of the piers. However, the prestressing bars could lose part of their tension over time due to effects like creep and shrinkage [14]. Especially during an earthquake, depending on the deformations that the structure suffers, it could be that the prestressing value is reduced, so it should be verified if this strengthening method is effective if the bars just act as passive reinforcement.

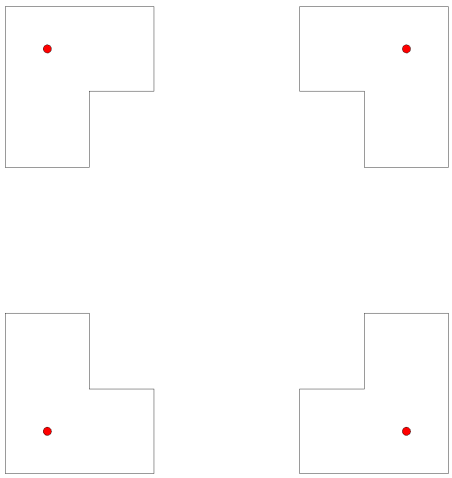

Figure 49: Introduction of the prestressing bars in the cross-section of the piers (in red)

A lot of thought has to be put into the anchoring of the prestressing. Indeed, the easiest way would be to anchor the bars just below the windows, so that the prestressing has to be introduced only in the upper part of the bell tower which has to be rebuilt anyway. They could be anchored for example in a reinforced concrete ring beam under the windows. However, by doing it this way, the lower part of the bell tower would not be prestressed and some other critical failure mechanisms could appear lower. Moreover, reinforced concrete elements introduced in the upper part of a structure often lead to higher seismic vulnerability, because of the high mass and stiffness compared to the masonry. Therefore, it would probably be

more ideal to have the prestressing on the whole height of the bell tower. This would require drilling vertical holes in the lower part of the bell tower, and would seriously complicate the anchorage of the prestressing, which would have to be done in the foundation somehow. It could potentially also lead to a very high axial load in the two columns that support the bell tower, which could become vulnerable. In this case the confinement of these columns could be a complementary action. The removability and invasiveness of this method would really depend on the anchorage system. Corrosion of the bars could also be a concern when it comes to durability.

Another alternative that can be considered is the addition of Fiber Reinforced Polymer (FRP) laminates on the masonry surface. In order to preserve the aspect of the church on the outside, this method would ideally be applied only on the inside of the tower, with vertically spanning laminates on the piers' internal faces (see figure 50). Cracks could still form on the outside, but the mechanism would not be able to develop thanks to the added tensile strength on the inside. Since there is not a very large surface to apply those laminates on the inside, structural analysis should be performed to check if the added tensile strength is enough. The FRP laminates would need to be extended on a certain length above and under the windows to have a sufficient anchoring length and to avoid the formation of other mechanisms higher or lower on the tower. This method does not increase the shear resistance of the piers, so its effectiveness would have to be verified. Another critical aspect with the implementation of this solution lies in the bond between the masonry and the strengthening material. The bond is provided by an epoxy resin, which can have some compatibility issues with the masonry [14]. A smooth and clean surface of the masonry is needed for a good bond. This method is hardly removable without damaging the masonry and somewhat invasive, but if limited to the inside of the tower it can be acceptable.

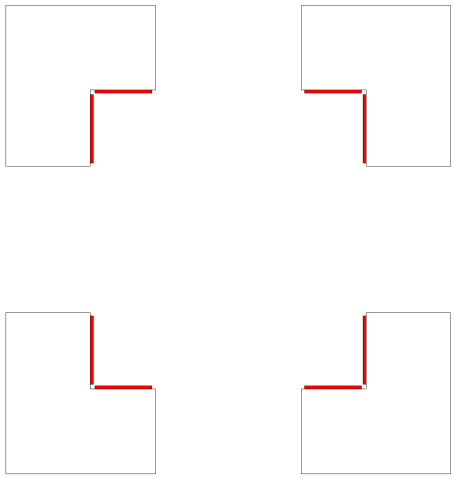

Figure 50: Application of the FRP laminates in the cross-section of the piers (in red)

6.3 Vaults

The vaults of the church suffered significant damage during the earthquake of 2020, with multiple cracks appearing in many locations. The pushover analyses also predicted cracking of the vaults, which indicates that some retrofitting measures are probably needed to avoid a complete collapse of the vaults during a future earthquake. Many different strategies can be applied to prevent the failure of vaults.

According to the ICOMOS-ISCARSAH Guidelines [17], the goal should always be to address the root of the problem. By looking at the results of the pushover analyses, it looks like the cracking of the vaults is caused by the displacement of an adjacent element, and not directly by the failure of the vaults themselves. Indeed, in the +X direction, the rocking of the bell tower pushes on the large vault which seems to cause the cracks. In the −X direction, cracks appear at the connection of the large vault with the bell tower because of the separation of the bell tower. And in the +Y direction, the out-of-plane movement of the northwest wall leads to the failure of the vaults, because the supports of the vaults are moving away from each other.

Therefore, before considering a retrofitting measure on the vaults themselves, it could be more effective to try to prevent the movement of the elements that support the vaults. Such measures could potentially avoid the cracking of the vaults without having to perform heavy interventions on the vaults, and would be in accordance with the principles of ICOMOS-ISCARSAH, i.e. treating the root of the problem and favoring the minimal intervention.

The separation of the bell tower and the vault predicted by the −X pushover analysis should already be solved with the introduction of steel ties described in section 6.1.

Concerning the problems brought forward by the +Y pushover analysis, the cracking of the vaults would be avoided if the OOP overturning of the northwest and southeast walls was restricted. A solution could be to introduce steel ties between these walls to withstand the thrust of the vaults and restrict the movement of the supports of the vaults. The best location to place them is probably at the center of the two central arches, where the thrust is the most important (see figure 51). Concerning the height, they could be introduced either under or over the arches. Placing the tie under the arch has the advantage of directly taking up the thrust of the arch, but it would be visible from inside the church and could be considered obtrusive. With a placement over the arch, the tie would not be visible but it would create a bending moment in the walls and a different failure mechanism could be possible [2] (see figure 52). A structural analysis would be necessary to determine which placement is more suitable. As already discussed for the ties in the other direction (section 6.1), this method provides a good compatibility, is removable and the durability should not be too much of a concern as most of the ties would be controllable.

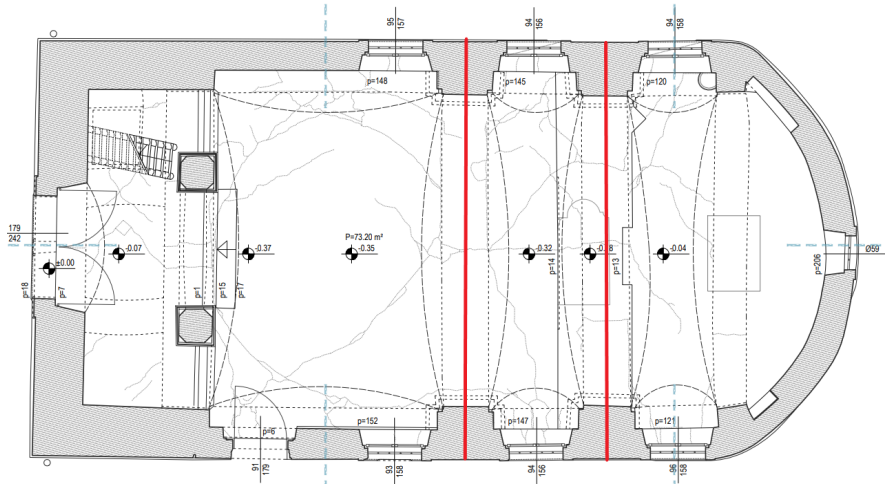

Figure 51: Introduction of the transverse steel ties

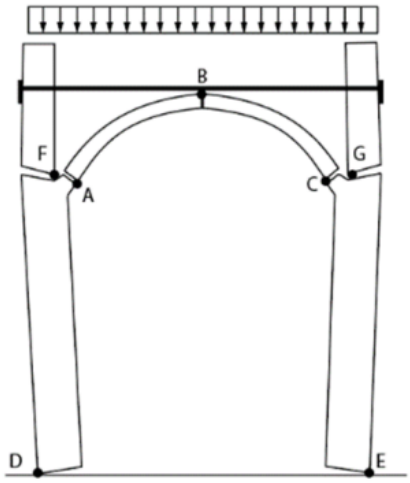

Figure 52: Possible failure mechanism with tie above the arch [2]

For the cracks predicted by the +X pushover analysis, the choice of a good retrofitting method is not as obvious. The goal would be to restrict the pushing of the bell tower against the vault. This could maybe be achieved with a rigid beam at the connection of the vault with the bell tower (above the two columns). This way, the rigid beam could withstand the thrust of the bell tower, which would not be transmitted to the vault. The choice of the material for this beam should be investigated deeply, but steel or concrete could be considered. The compatibility of the old and new materials would be a big challenge should this solution be implemented, since the addition of heavy and rigid elements like concrete or steel often leads to stress concentrations and can sometimes even worsen the seismic behaviour. This method also has the disadvantage of being hardly removable.

Should these methods not be satisfactory, it could still be possible to retrofit the vaults

directly. A good solution is the addition of composite materials such as Fiber Reinforced Polymer (FRP) laminates or Fiber Reinforced Cementitious Matrix (FRCM) on the extrados of the vaults [16]. This provides tensile strength on the extrados and allows the line of thrust to go outside the thickness of the vault. The provided tensile strength would avoid the formation of cracks on the extrados. Cracks could still appear on the intrados, but this would not be enough to form a mechanism and lead to the collapse of the vault.

Both the FRP laminates and the FRCM achieve the same goal and work in a similar manner, but the FRCM is chosen because of its good compatibility with the masonry material. Indeed the FRP laminates are bonded to the masonry surface with an epoxy resin, which is not as chemically compatible with the masonry as the cementitious matrix [16].

The choice of applying the FRCM on the extrados, instead of the intrados or both, has two reasons : on the extrados the intervention is not visible, therefore it is less invasive ; and if applied on the extrados, the tension in the fibers causes a compressive stress perpendicular to the masonry surface, while on the intrados it creates a tensile stress, which is obviously not ideal for masonry [14] (see figure 53).

Figure 53: Behaviour of FRCM at intrados and extrados of vaults [14]

7 Further investigations

The seismic assessment of the church that was presented in this report is not yet complete and could really benefit from further investigations. Indeed, this project was limited in time and it would be possible and interesting to go more in detail in many aspects of the analysis if more time was on hand.

First of all, in order to get more precise results it would be very important to reduce the uncertainties about the material properties. Some estimations made in the analysis were pretty rough and as it was addressed in section 4.4.5, some parameters like the tensile strength have a big influence on the results. It would be interesting to do some sensitivity analyses on some parameters to identify the ones that have the biggest influence on the results. Then, these parameters should be investigated in depth to get accurate estimations, probably with the help of tests carried out on the material of the church.

Some improvements could also be done on the numerical model. The biggest improvement would be to model the church with 3D solid elements instead of 2D shell elements. The model would be much more accurately representing the geometry of the church and less simplifications would be needed. The out-of-plane behaviour would probably be captured more precisely as well. Eliminating a few simplifications that were used (e.g. modelling of the apse with three straight segments, shape of the windows) would be another direction to investigate. Finally, it could be interesting to model the roof and the spire entirely, instead of just adding their masses to the model, and analyse the influence that this simplification has on the numerical simulation.

The application of the N2 method to an irregular building as a church has brought a few difficulties. Indeed, the mode shapes do not always correspond well to the deformed shapes coming from the pushover analyses. As it was mentioned in section 4.4.5, an improvement could be done by using the deformed shape from a pushover analysis on a linear elastic system instead of the modal shape. To go even further, a dynamic analysis could be performed, which would probably provide more accurate results, as the static pushover analysis appears to reach its limits for irregular building shapes.

Finally, the retrofitting of the church was only addressed partially. Retrofitting solutions were proposed and discussed for a few critical points of the structure, but further analyses would really be necessary before considering the implementation of any of those interventions. More precise results would already be needed for the unretrofitted structure in order to identify the parts that really need strengthening and the ones that do not. This could be achieved with the refinements of the model discussed above. Then, the effects of the retrofitting strategies should be investigated by implementing them in the model, and only then it could be concluded if a proposed retrofitting solution is effective and adequate for this church or not.

8 Conclusion

In this work, a seismic assessment of the Kapela Sveti Nikola in Petrinja was done, and retrofitting measures were proposed for a few critical elements of the church. The study of this particular case can provide some useful information for other seismic evaluations of unreinforced masonry churches, especially because the results of the analysis can be compared to the actual behaviour of the church during the earthquake.

The first lesson we can learn from this project is that obtaining accurate and trustworthy results from a static pushover analysis on a building whose geometry is as irregular as a church is complicated. Compared to a building that is very regular in plan and elevation, where the fundamental mode is really predominant, a church's seismic behaviour is also influenced significantly by the higher modes, as it was shown in the modal analysis (section 4.4.1). And the N2 method, which is used to compare the capacity and the demand when performing static analysis, only considers the first mode, therefore its application is not as straightforward and reliable.

In addition, this work really showed the influence that the material properties can have on the results. As illustrated in section 4.4.5, the modification of a single parameter like the tensile strength can have a decisive influence on the load capacity, the displacement capacity and even on the nature of the failure mechanism. It is therefore crucial to estimate these properties as accurately as possible, if needed with the help of tests on the material of the building. Every masonry building has its own unique materials, whose properties are also evolving over the lifetime of the building, influenced by many effects (chemical, meteorological, mechanical etc.). Consequently, reliable estimations of the masonry properties are difficult to obtain from codes or literature, and experimental testing on the building's materials seems to be the best way to reduce the uncertainties of the material properties.

Despite this, the seismic assessment that was carried out still allows to get a reasonably good idea of the seismic performance of the church. Especially the failure mechanisms predicted by the pushover analysis seem to make sense, and similarities can be found in many places with the damage reported on the church. Even though nonlinear dynamic analysis seems necessary to get really precise results, it can still be a good idea to perform a pushover analysis and hand calculations in the early stages of a project, to get a first estimation of the performance of the structure.

Concerning the retrofitting measures, a more precise seismic assessment would again be needed to really justify any intervention. However, the damage predicted in the analyses and observed on the church allow to identify some of the most critical parts of the structure, where strengthening actions are probably necessary. The reflections on the retrofitting of this church really underline how crucial it is to consider from the beginning of the process not only the structural aspect, but also the conservation of the cultural value of any historical building. Balancing all the criteria that influence the choice of a retrofitting strategy is a challenging task that should not be underestimated.

References

[1] K. Beyer. Civil-522 - seismic engineering. Course presentations, EPFL, 2022.

[2] G. Cianchino, M. Masciotta, C. Verazzo, and G. Brando. An overview of the historical retrofitting interventions on churches in central italy. *Applied Sciences*, 2023.

[3] Ministero delle Infrastutture e dei Trasporti. Istruzioni per l'applicazione dell'«aggiornamento delle "norme tecniche per le costruzioni"» di cui al decreto ministeriale 17 gennaio 2018. *Gazzetta Ufficiale*, 2019.

[4] L. Diana, G. Vaiano, A. Formisano, L. Scandolo, S. Podestà, and P. Lestuzzi. The seismic vulnerability assessment of heritage buildings: A holistic methodology for masonry churches. *International Journal of Architectural Heritage*, 2023.

[5] European Committee for Standardization. *Eurocode 8: Design of structures for earthquake resistance - Part 1 : General rules, seismic actions and rules for buildings*, 2004.

[6] European Committee for Standardization. *Eurocode 8: Design of structures for earthquake resistance - Part 3: Assessment and retrofitting of buildings*, 2005.

[7] European-Mediterranean Seismological Centre. *M 6.4 - CROATIA - 2020-12-29 11:19:54 UTC*, 2020. Available : `https://www.emsc.eu/Earthquake/earthquake.php?id=933701#summary`.

[8] P. Fajfar. A nonlinear analysis method for performance based seismic design. *Earthquake Spectra*, 16(3):573–592, August 2000.

[9] M. Gams, A. Penna, P. Morandi, F. Vanin, and K. Beyer. European database on masonry wall tests, 2018. Available : `https://zenodo.org/record/6224940#.Yl_SfInP3D4`.

[10] M. Godio and K. Beyer. Evaluation of force-based and displacement-based out-of-plane seismic assessment methods for unreinforced masonry walls through refined model simulations. *Earthquake Engineering Structural Dynamics*, 2018.

[11] M. Herak. *Karte potresnih područja Republike Hrvatske*. Geofizički odsjek Prirodoslovno-matematički fakultet Sveučilišta u Zagrebu. Available : `http://seizkarta.gfz.hr/hazmap/karta.php`.

[12] H. Kaushik, D. Rai, and S. Jain. Stress-strain characteristics of clay brick masonry under uniaxial compression. *Journal of Materials in Civil Engineering*, 19(9):728–739, 2007.

[13] P. Lourenço and A. Gaetani. *Finite Element Analysis for Building Assessment*. Routledge, 2022.

[14] NIKER Project. *Deliverable 3.2 - Critical review of retrofitting and reinforcement techniques related to possible failure*, 2010.

[15] J. Prtoric. Après un nouveau séisme en croatie, la détresse. *Libération*, December 2020. Available : https://www.liberation.fr/planete/2020/12/29/apres-un-nouveau-seisme-en-croatie-la-detresse_1809924/.

[16] G. Ramaglia, G. Lignola, and A. Prota. A simplified approach to evaluate retrofit effects on curved masonry structures. Technical report, Department of Structures for Engineering and Architecture, University of Naples Federico II, Italy, 2015.

[17] P. Roca. *The ISCARSAH Guidelines on the Analysis, Conservation and Structural Restoration of Architectural Heritage*. ICOMOS-ISCARSAH, 2020.

[18] Z. Salat. Numerical modelling of out-of-plane behavior of masonry structural members. Master's thesis, Technical University of Catalonia, 2015.

[19] Seismological Survey of Croatia, Faculty of Science, University of Zagreb. *Razoran potres kod Petrinje*, 2020. Available : https://www.pmf.unizg.hr/geof/seizmoloska_sluzba/izvjesca_o_potresima?@=1m68n#.

[20] Société suisse des ingénieurs et des architectes. *SIA 266 - Construction en maçonnerie*, 2015.

[21] Société suisse des ingénieurs et des architectes. *SIA 261 - Actions sur les structures porteuses*, 2020.

[22] M. Tomazevic. Shear resistance of masonry walls and eurocode 6: shear versus tensile strength of masonry. *Materials and structures*, 2009.

[23] M. Uroš, M. Demšić, M. Šavor Novak, J. Atalić, and S. Prevolnik. *POTRESNO INŽENJERSTVO - Obnova zidanih zgrada*. Građevinski fakultet Sveučilišta u Zagrebu, 2021.